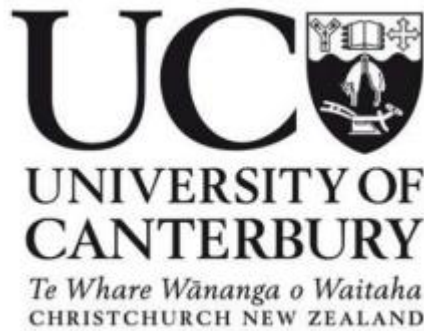


Effects of abiotic stress on the oomycete

Phytophthora pluvialis.



A thesis submitted in partial fulfilment of the requirements for the Degree of

Master of Science in Biotechnology

in The University of Canterbury

by Leann Seesom Vinson

University of Canterbury

2022

Abstract

Phytophthora pluvialis (*P. pluvialis*) is the causative agent of red needle cast (RNC) disease in radiata pine. Currently, RNC is seen as a cause of concern in the North Island but is trickling its way down into the South Island. This could widely impact New Zealand's economy, as the export of pine wood approximates \$6.7 billion or 1.6% of the country's overall GDP.

Studies published on *P. pluvialis* are aimed towards identifying movement of the disease, elimination strategies, identification methods and deriving genomic data during infection. Not much is known about the impacts of abiotic stress caused by climate change on the disease. In this research, I investigate the optimal growth temperature, effects of drought and salinity stress on the growth rate of several *P. pluvialis* strains. First, 21°C was identified as the temperature with the highest mycelial growth, for the following five different *P. pluvialis* strains; 3000, 3618, 3632, 3880 and 4015. Secondly, the growth rate of mycelium was quantified during 7 days of exposure to drought and salinity stress, using varying concentrations of polyethylene glycol (PEG) and sodium chloride (NaCl), respectively. Finally, bZIP transcription factor family known to be involved in oxidative stress in *P. infestans* was analyzed in detail for *P. pluvialis* using a computational approach including phylogenetic analyses and protein modelling to determine conserved regions.

Acknowledgements

First, I would like to thank my supervisor, Claudia Nicole-Meisrimler for helping me through this research through all the obstacles I have faced during this year. Thank you so much for giving me the opportunity to explore and navigate the world of research even while being so far away.

This year has not been easy with the COVID-19 pandemic, not being able to travel and visit my family back home. I would like to thank my parents, Timothy and Israpon for giving me the opportunity to study in New Zealand and being my rock every step of the way. I would also like to thank my brother, Lucas for always bring a smile on my face on particularly bad days.

Thank you to my friends who have been with me through the good, bad, and ugly times.

Table of Contents

Introduction	12
1.1. <i>Phytophthora pluvialis</i>	12
1.1.1. Overview	12
1.1.2. Genetic background.....	13
1.1.3. Life cycle and Morphology of <i>Phytophthora</i>	14
1.2. <i>P. pluvialis</i> hosts.....	17
1.3. Significance and current control management	17
1.4. Abiotic stress on plants.....	19
1.4.1. Phenotypic responses to abiotic stress in plants	20
1.4.2. Immune responses to abiotic stress in plants.....	21
1.5. Abiotic stress effects on filamentous pathogens.....	21
1.6. bZip transcriptional factors.....	23
1.7. Research questions and hypothesis.....	24
1.8. Research purpose.....	24
Chapter 2. : Materials and methods.....	26
2.1. Maintenance of <i>P. pluvialis</i> on V8 media	26
2.2. <i>P. pluvialis</i> : Determining optimum growth temperature	26
2.3. <i>P. pluvialis</i> under salinity and drought stress	27
2.4. Abiotic stress effects on mycelium growth for quantitative PCR (qPCR) analysis	28
2.5. Primer design.....	29
2.5.1. <i>Phytophthora pluvialis</i> primers for genes of interest	29
2.5.2. Internal standard primers for <i>P. pluvialis</i> actin and COX2	30

2.6.	RNA extraction and reverse transcription	30
2.7.	PCR.....	31
2.7.1.	Primer reactivity and specificity.....	31
2.8.	Reverse transcriptase quantitative PCR (qPCR).....	32
2.8.1.	Primer efficiency	34
2.9.	Phylogenetic analysis	34
2.10.	Protein modelling	35
Chapter 3.	Results	36
3.1.	Determining <i>P. pluvialis</i> optimum growth temperature	36
3.2.	<i>P. pluvialis</i> growth rate under abiotic stress.....	38
3.2.1.	Salinity.....	38
3.2.2.	Drought.....	41
3.3.	Primers and PCR	44
3.4.	RNA and cDNA preparation	46
3.5.	Reverse transcription quantitative PCR.....	47
3.5.1.	PpR01 primer binding efficiency in <i>P. pluvialis</i> mycelium samples	47
3.5.2.	Actin efficiency	49
3.5.3.	Expression of PpR01 under salinity and drought stress	50
3.5.4.	Expression of bZIP, PPZIP_07, under salinity and drought stress.....	50
3.6.	Phylogenetic analysis	51
3.6.1.	Conserved <i>P. pluvialis</i> and <i>P. infestans</i> bZIP transcription factors.....	51
3.6.2.	Phylogenetic similarities.....	53
3.6.2.1.	bZIP family conservation of <i>P. pluvialis</i> and <i>P. infestans</i>	53
3.6.2.2.	bZIP family in <i>P. pluvialis</i> and closely related ancestors.....	54

3.7. Protein models	54
Chapter 4. Discussion.....	57
4.1. Mycelium growth	57
4.2. Expression of PpR01 and bZIP under abiotic stress.....	59
4.3. Phylogenetic analysis of <i>P. pluvialis</i> bZIPs	60
Chapter 5. Conclusion.....	63
5.1. Future directions.....	63
5.2. Concluding remarks.....	63
Bibliography	65
Supplemental	74

List of figures

Figure 1: Map visualising presence of <i>P. pluvialis</i> in the World, CABI 2022.....	14
Figure 2: Overview of <i>P. pluvialis</i> reproduction and <i>Phytophthora</i> phylogenetic tree.....	16
Figure 3: Phenotypic variation of Masson pine seedlings under different soil moisture conditions.....	20
Figure 4: Process of harvesting and growing mycelium in liquid V8 broth.....	29
Figure 5: Various strains of <i>P. pluvialis</i> grown at temperatures 21°C	37
Figure 6: <i>P. pluvialis</i> grown at 15°C-21°C.....	38
Figure 7: <i>P. pluvialis</i> grown on V8 media under salinity stress	40
Figure 8: Analysis of <i>P. pluvialis</i> under salinity stress	41
Figure 9: <i>P. pluvialis</i> grown on V8 agar media under drought stress	43
Figure 10 :Analysis of <i>P. pluvialis</i> under drought stress.....	44
Figure 11:Gel electrophoresis of primers tested for PpR01, <i>P. pluvialis</i> actin and <i>P. pluvialis</i> BZIP TF	45
Figure 12: Standard curve of PpR01	48
Figure 13: Standard curve of PACT-1.....	49
Figure 14: Expression of PpR01 during salinity and drought stress induced by NaCl and PEG, respectively.	50
Figure 15:Expression of bZIP during salinity and drought stress induced by NaCl and PEG, respectively.....	51
Figure 16 : RAxML tree of <i>P. pluvialis</i> and <i>P. infestans</i> bZIPs	54
Figure 17 : Analysis of PPZIP 14.....	53
Figure 18 : Protein models of <i>P. pluvialis</i> bZIP transcription factor homodimers by AlphaFold2.....	55
Figure 19: Analysis of <i>P. pluvialis</i> PPZIP 14.....	56

List of tables

Table 1: Replicates table for optimal temperature test	27
Table 2: Replicates table for PEG and NaCl treatments.....	28
Table 3: PCR setting.....	31
Table 4: Serial dilution table of cDNA for qPCR.....	32
Table 5: Plate map for qPCR pipetting.....	33
Table 6: qPCR settings	33
Table 7: Primer chosen from gel electrophoresis	45
Table 8: Selected primers and their base pair lengthss.....	45
Table 9: RNA concentrations from Nanodrop and Qubit Fluorometer 2	46
Table 10 : cDNA dilution table.	47
Table 11: <i>P. infestans</i> bZIP with renamed <i>P. pluvialis</i> bZIP.	52

Abbreviations

RNC: Red needle cast

TFs: Transcriptional factors

PEG: polyethylene glycol

PpR01- *Phytophthora pluvialis* RxLR effector protein-1

PACT-1: *Phytophthora pluvialis* actin primer-1

bZIP: Basic leucine zipper protein

ITS: Internal transcribed spacer region

MAPK: mitogen-activated protein kinase

JA: jasmonic acid

ABA: abscisic acid

SA: salicylic acid

PAMP: Pathogen associated molecular pattern

PRI: PAMP/Pattern triggered immunity

ETI: Effector triggered immunity

PRR: pattern recognition receptors

Introduction

1.1. *Phytophthora pluvialis*

1.1.1. Overview

Phytophthora pluvialis (*P. pluvialis*) is an oomycete class pathogen. Oomycetes are filamentous eukaryotic microorganisms closely related to photosynthetic algae, previously thought to be part of fungi [1]. Currently, oomycetes are classified under the Kingdom Chromista or Stramenopila and are commonly known under the name “plant destroyers.” They are characterized by their zoospores, which have two distinct types of flagellum, anterior and posterior, attached to a ventral groove [2]. There are approximately 100 known species and potentially 500 unknown species of *Phytophthora*. The first *Phytophthora* species, *Phytophthora lateralis*, was isolated from roots and collars of ornamental cedars and causes cedar root rot in Lawson cypresses (*Chamaecyparis lawsoniana*); which was followed by the discovery of numerous *Phytophthora* species [3–5]. *Phytophthora* species can be soil, air and water borne with a hemibiotrophic or necrotrophic lifestyle. Their spread mostly associates with the movement of infected plants, contaminated soil, and natural disasters [6]. Different *Phytophthora* species are associated with various diseases such as, late potato blight (*Phytophthora infestans*), sudden oak death (*Phytophthora ramorum*) and kauri dieback (*Phytophthora agathidicida*). These diseases have caused damage to natural ecosystems, raised global food security concerns and economic concerns for countries that rely on the import and export of these plants and their production [7].

In New Zealand, many plant pathogens belong to the genus *Phytophthora*, including *P. pluvialis*. *P. pluvialis*, the causative agent of red needle cast (RNC), has been observed on various species of pine trees. The first sighting of RNC in New Zealand was in 2008 on the North Island [8]. In New Zealand, RNC infestation has been linked to the import of contaminated trees and farming equipment imported from Oregon, USA [9]. The disease was first sighted on both Monterey pine (*Pinus radiata*) and Douglas-fir (*Pseudotsuga menziesii*), where it causes black resinous bands on needles and olive-

coloured lesions followed by accelerated senescence and casting that occur in autumn and spring months when the weather tends to be damp and cold [8]. Like other *Phytophthora* spp., *P. pluvialis* thrives and reproduces in wet or damp environments [10].

In the laboratory environment, *Phytophthora* spp. are grown in carrot broth or carrot agar, alternatively, it is also done using V8 broth or agar [11]. In recent years, V8 media has been the default choice for oomycete culturing. Due to its clarity and ingredients, it allows oomycetes to be easily identifiable on a macroscopic and microscopic scale [12]. Macroscopically, *P. pluvialis* mycelium appears to grow in regular pattern that is seen in other *Phytophthora* spp., a steady growth rate is first seen followed by a second wave that causes mycelium to grow vertical to the media. Microscopically, other structures such as, mycelium, hyphae and sporangia share similar appearance to *Phytophthora* spp.

1.1.2. Genetic background

The origin of *P. pluvialis* is theorised to be from the Pacific Northwest Coast region of the United States of America (USA), which includes Washington, Oregon, and California. These states are native habitats to Douglas fir (*Pseudotsuga menziesii*), Tanoak (*Notholithocarpus densiflorus*) and Monterey pine (*Pinus radiata*). Studies focusing on comparing the genetic diversity of *P. pluvialis* in USA versus New Zealand, using single nucleotide polymorphism (SNP) and multilocus genotypes (MLGs) have indicated that *P. pluvialis* has twice the genetic diversity in the USA when compared to the New Zealand population [13]. The two genetic clusters found in New Zealand, NZ1 and NZ2, are genetically distinct from each other. However, NZ2 shows more genetic similarity to the US cluster, therefore, indicating two points in time when *P. pluvialis* was introduced to New Zealand [14]. Genetic variation is not limited to just these two countries. Further studies in the USA indicated less genetic differentiation between neighbouring states as opposed to states further apart, which seen to increased genetic diversity. This was also observed in neighbouring regions in New Zealand and indicates that mutations might occur due to *P. pluvialis* developing adaptations to local weather conditions and colonial expansion [14].

In late 2021, *P. pluvialis* was discovered in the UK and was identified in the England, Scotland and Wales [15]. The Invasive Species Compendium has been recently updated and currently shows that *P. pluvialis* is present in the United States of America, the United Kingdom (UK), and New Zealand. Studies are underway to confirm if *P. pluvialis* present in Europe is genetically similar to currently known species.

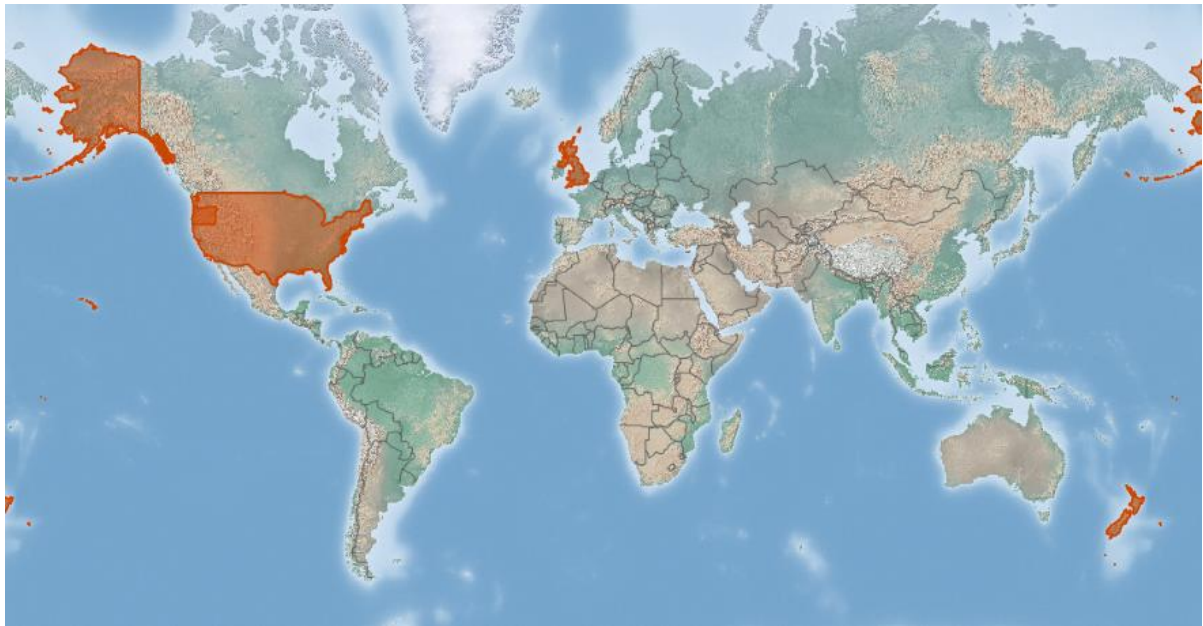


Figure 1: Map visualising presence of *P. pluvialis* in the World, CABI 2022. *Phytophthora pluvialis*; Highlighted red regions show the presence of *P. pluvialis* around the world. Currently in the U.S.A, UK, and New Zealand.; In: *Invasive Species Compendium*. Wallingford, UK: CAB International. <https://www.cabi.org/isc>

1.1.3. Life cycle and Morphology of *Phytophthora*

Currently all known *Phytophthora* spp., have a similar life cycle. *Phytophthora* spp. show phenotypic plasticity, by developing mechanisms and structures when exposed to a change in the surrounding environment. Two main structures are necessary for all *Phytophthora* spp. survival, these are: chlamydospores and oospores. These spores are produced during the asexual and sexual phase, respectively. In the asexual phase, sporangiophores are simple or sympodial with irregular ovoid shaped sporangia attached. Chlamydospores germinate to form sporangia, in water sporangia are semi-

papillate, terminal or subterminal with an average size of 53-67 μM by 39-45 μM . Hyphae networks are present with globose, intercalary hyphal swellings at the tips. During the sexual phase, oospores are globose and aplerotic with an average size of 27-29 μM . Hyphae are globose and smooth, comprising of a terminal oogonia with amphigynous or paragynous antheridia and are approximately 27-34 μM in size [16,17].

During damp conditions spores germinate and eventually develop into sporangia that release single celled, biflagellate zoospores that are approximately 10-17x7-12 μM in size [18]. Zoospores are sensitive, prone to drying, therefore, move in damp soil or leaves and finally attach to susceptible plants root or leaves. Once attached, a cyst is formed, these cysts germinate and produce thread-like structures called hyphae. Hyphae boar into the plants cells to obtain nutrients. Finally, producing chlamydospores and oospores, thus repeating the cycle. *Phytophthora* spp. are considered hemi-biotrophic with a part of the life cycle being symbiotic or biotrophic followed by a necrotrophic phase, draining the plant of all its resources [19,20].

Phytophthora spp. were first categorised into clades using internal transcribed spacer regions (ITS), other studies have also used nuclear genes, mitochondrial genes, and nuclear genetic markers to phylogenetically analyse the relationship between species [4,8,21,22]. There are 10 ITS cades currently known for *Phytophthora* spp.; each clade is morphologically similar. Genome sequencing has placed *P. pluvialis* under ITS Clade 3, which also includes, *Phytophthora psychrophilia*, *Phytophthora ilicis*, *Phytophthora nemorosa* and *Phytophthora pseudosyringae* [23].

While being morphologically similar, *P. pluvialis* is easily differentiated from the other *Phytophthora* spp. in ITS clade 3. On average, it produces larger sporangia and has distinct hyphal swellings in water and agar. The size of its oogonia and oospores are mid-sized compared to the larger *P. pseudosyringae*

and *P. ilicis* and smaller than *P. nemorosa* and *P. psychrophila* [16]. On agar media, the colony patterns of all ITS clade 3 *Phytophthora* spp. are nearly identical.

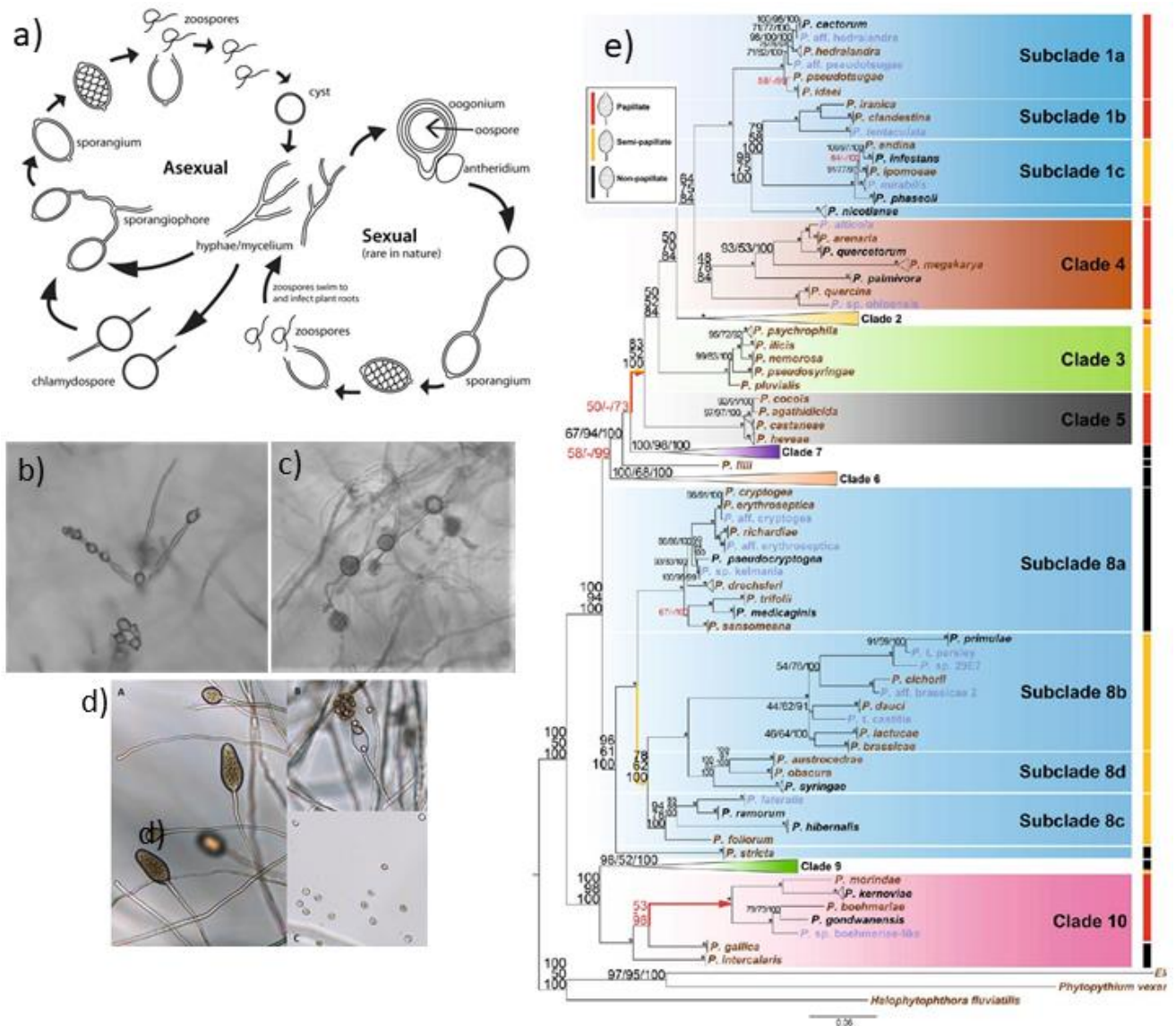


Figure 2: Overview of *P. pluvialis* reproduction and *Phytophthora* phylogenetic tree a) Asexual and sexual reproduction of oomycetes. Image by: G. Abad, T. Burgess, J.C. Bienapfl, A.J. Redford, M. Coffey, L. Knight; from: https://idtools.org/id/phytophthora/about_phytophthora.php; b) Microscopic image of *P. pluvialis* sporangia; c) Microscopic image of *P. pluvialis* chlamydospores; d) Microscopic image of mature sporangia releasing zoospores by : Sharma, M. and Ghosh, R. (2016). DOI: 10.21769; e) Phylogenetic tree of various *Phytophthora* species branches show bootstrap values. *Phytophthora pluvialis* is seen in Clade 3. Tree obtained from: Yang, X., Tyler, B.M. & Hong, C. An expanded phylogeny for the genus *Phytophthora*. IMA Fungus 8, 355–384 (2017) <https://doi.org/10.5598/imafungus.2017.08.02.09>

1.2. *P. pluvialis* hosts

The total number of hosts species that are susceptible to *P. pluvialis* infection are currently unknown. The first record of *P. pluvialis* was observed on the forest canopy, in soil and neighboring water sources surrounding a mixed Douglas-fir-tanoak forests in their native habitat of Curry County, Oregon, U.S.A. [16]. Later, *P. pluvialis* was isolated from Douglas-fir needles in several states along the west coast region of the USA [14,24].

During the 19th century, Monterey pine, also known as, Radiata pine was imported into New Zealand from its native region of California, U.S.A., to be used in forestry and timber production [25]. In 2008, RNC was observed for the very first time on imported Radiata pine, six years later, *P. pluvialis* was identified as the cause of the RNC [8]. Further molecular and genomic studies following the initial discovery of *P. pluvialis* in New Zealand, have allowed for better detection and identification of the pathogen [11,26].

As mentioned in *Section 1.1.2*, *P. pluvialis* has been recently identified in the UK and was observed infecting a novel host, the Western Hemlock (*Tsuga heterophylla*), during a routine surveillance of *Phytophthora ramorum* [27]. It has now been confirmed to be present in parts of England, Scotland and most recently Wales [15,28].

1.3. Significance and current control management

In 2018, the forestry industry in New Zealand was worth approximately \$6.7 billion or 1.6% of the country's overall GDP, it is one of the largest products exported, third to the dairy and meat industry (4%). In fact, 90% of trees planted in New Zealand are *P. radiata*, the remaining is made up of Douglas-fir and other species[29]. On an international perspective New Zealand contributes to a small percentage of 1.1% to the world's total supply of industrial wood and 1.3% of the worlds trade in forest products, however, it is predicted to rise in the future [30]. A record 35.4 million cubic metres of timber was

harvested in 2018, an increase of 10% on the previous year. Volumes are expected to be comparable for the next decade until 2030, as forests planted in recent decades reach maturity. The products are exported to countries such as China, Australia, the Republic of South Korea and Japan [31,32]. Contaminated or low-quality products exported to these countries could cause a loss in the local GDP of the country. In addition, the forestry industry stimulates local economy and supporting for over 35,000 local jobs in New Zealand in various sectors of wood production, processing, and commercial sector.

Today, there are three methods that are currently being used to prevent the spread of *P. pluvialis*. These methods are breeding resistant plant, chemical and biological control [33]. Breeding for resistance needs to consider several factors, including tolerance of the pine to stress factors, growth rates for reliable production in context with the risk of RNC. *P. pluvialis* infection is dependent on environmental conditions and climatic factors, which is difficult to inoculate in laboratory settings or even within field trials. To be able to develop resistant plants, artificial inoculation *in planta* assays using *P. pluvialis* zoospore suspensions is used. The limitation to this method, however, is that zoospore encysts become ineffective if not prepared in rigorous conditions and used within 2 hours [33]. For the chemical control method, *P. radiata* is sprayed with phosphite (phosphorus acid) prior to detection of infection or once signs of RNC is detected [34–36], resulting in the reduction in the length of lesions on infected needles. Limitations of this method are due to *P. pluvialis* being airborne and distributed in water droplets this means that trees in the surrounding area that are not sprayed are potentially infected developing RNC. Additionally, this method of treatment is expensive and brings about environmental and social concerns in local communities. Alternatively, copper oxychloride and phenylamine metalaxyl-M are also used as effective fungicides. The use of chemical fungicides is dependent on pathogen identification and understanding disease epidemiology [8]. On the other hand, biological control method involves the identification and screening of biological agents against *P. pluvialis*. Studies have shown that arbuscular mycorrhizal, *Pseudomonas spp.* and *Trichoderma spp.*, have been affective biological agents against *Phytophthora spp.* [37–39].

1.4. Abiotic stress on plants

Plant disease can be defined as any physiological disruption or function of the plant [40]. Plants are susceptible to a multitude of predators and pathogens that can lead to destruction and ultimately death. To counter biotic stresses, plants have developed an innate immune system. Two main factors activate an immune response, these are biotic agents such as herbivorous animals, insects, bacteria, and fungi. Interestingly, also abiotic factors such as temperature change, nutrient deficiency, drought, pollution, heavy metals, and ultraviolet radiation can trigger plant immunity [41,42]. Seasonal crops are sensitive to abiotic stress and therefore do not have complex mechanisms to prevent their senescence and need to be selectively bred for stress resistance over time, on the other hand, trees are sessile and have adaptation and recovery mechanisms during varying weather conditions [43,44].

The cause of drought stress is insufficient water availability to the plant and occurs due to various environmental factors, including arid weather conditions, low rain fall, and high salinity. Drought stress adaptation associates with well-studied physiological processes, including, stomatal closure to prevent water loss. However, in trees like in other plants this does not fully prevent the water loss [45]. Excessive water loss can lead to a xylem embolism and therefore inefficient uptake and distribution of water throughout the plant [46]. In addition to stomatal closure, trees have morphologically adapted to produce smaller leaves or needles, waxy cuticles, a longer and deeper root systems allowing them to manage water loss more efficient than vegetable plants [35,47,48].

Nevertheless, excessive water loss can lead to a xylem embolism and therefore inefficient uptake and distribution of water throughout the plant [46]. Furthermore, prolonged water limitation can lead to mineral deficiency with longer-term effects on the overall tree health. Osmotic stress is considered a “sister” stress factor of drought. This is based on the fact that the drought stress’s associated water limitation leads to decreased water to solute ratio – leading to osmotic stress. Osmotic stress has been studied over decades in vegetable crops, but our understanding of its effects on trees is still limited [47,49]. High soil salt salinity has been studied mostly for an abnormally high amount of NaCl which

leads to an imbalance in ions. Osmotic stress has been shown to lead to increase in reactive oxygen species (ROS) leading to an ion-related cell damage [50–52]. During salinity stress stomatal closure and shoot cell expansion occurs followed by early onset senescence and cell death caused by cytotoxicity[49,53]. Salinity adaptations to maintain ion concentrations in the cytoplasm, include the release of excess Na⁺ into the soil, nitric oxide which activates antioxidant production for detoxification, polyamine production to reduce ROS production and compartmentalisation of ions which include the accumulation of Cl⁻ in root vacuoles, accumulation of ions in older sacrificial tissue [54–58]. Both, drought and osmotic stress, induce reactions comparable to the activation of the innate immune system. How far these adaptation pathways are linked is not clear at present and needs to be further investigated.

1.4.1. Phenotypic responses to abiotic stress in plants.

Abiotic stresses show similar signs of deterioration and degradation in various crops and trees. Early signs of drought, salinity or water stress are wilting, yellowing, and rolling of leaves which eventually leads to the defoliation of leaves. These initial signs are usually recoverable once conditions return to optimum. Long-term effects of drought include sparse foliage, drying and necrosis in leaves, branch death in the outer most regions of the tree, bark crack, stunted growth, stunted healing, suitability to pest infection and ultimately death [48,59].



Figure 3: Phenotypic variation of Masson pine seedlings under different soil moisture conditions. CK, well-watered control; LD, light drought; MD, moderate drought; and SD, severe drought. Figure obtained from Du M, Ding G, Cai Q. The Transcriptomic Responses of *Pinus massoniana* to Drought Stress. *Forests*. 2018; 9(6):326. <https://doi.org/10.3390/f9060326>.

1.4.2. Immune responses to abiotic stress in plants.

To adapt to stress conditions, plants have developed regulatory mechanisms, involving functional and regulatory proteins, that induce cross-talk between molecular and biochemical processes and altering gene expression and signal transduction pathways [60,61]. During initial exposure to abiotic stress, a non-specific defense response is triggered, PAMP (pathogen associated molecular patterns) triggered immunity (PTI). PTI occurs when cognate pattern recognition receptors (PRR) on the plant cell membrane are activated in the presence of pathogen or abiotic stress. The presence of abiotic stress triggers an immune response from the plant, which includes an initial Ca^{2+} ion flux across membranes, the production of reactive oxygen species (ROS) and phosphorylation cascades of mitogen-activated protein kinase (MAPK), production of callose against the cell wall [62,63] and the accumulation and signalling of phytohormones, salicylic acid (SA), ethylene, jasmonic acid (JA) and abscisic acid (ABA). Phytohormones accumulation is specific to the type of abiotic response present, SA is present during heat, ozone and UV light stress, ethylene during hypoxia, JA and ABA during drought, salinity, cold and heavy metal[64–67]

1.5. Abiotic stress effects on filamentous pathogens

Fungi and oomycetes are filamentous pathogens have been termed infamously as “plant destroyers” when left untreated. Both filamentous pathogens share similar lifestyles and phenotype but are morphologically distantly related. During the initial infection stage, the effects to the plant are minimal and include a decrease in yield, stunted growth, increase susceptibility to secondary infection and abiotic stress, in later stages, the pathogen switches to a necrotrophic lifestyle causing senescence [68]. Most *Phytophthora* spp. of oomycetes are obligate biotrophs or hemibiotrophs.

Fungi and oomycetes invade host cells by secreting and translocating effector proteins into the host apoplast and symplast, nevertheless, morphological differences exist on the cellular level on the interaction [69]. The host’s detection of effectors in plant cells triggers an initial immune response,

effector triggered immunity (ETI). However, effectors can disrupt PRR and PTI, when unrecognized which leads to deregulation or suppression of the host immune responses. Plants containing the resistance gene (R-gene) can trigger effector triggered immunity (ETI) when PTI is disrupted and activate a hypersensitive response (HR) which contains, and isolates spread of infection by inducing cell death in infected cells. Cross tolerance of plants during biotic and abiotic stress is dependent on the plant species, age, size and plant and pathogenic genotype [70].

The exposure to abiotic stress and subsequently its effects on pathogens, is dependent on the type pathogen being studied, as well as, adaptations of certain strains. An increase in environmental temperature tends to favour pathogenicity as opposed to lower temperatures, with the exception of adapted pathogens. An example of increased pathogenicity at higher temperature is seen in, *Pseudomonas syringae* DC3000. *P. syringae* DC3000 effectors translocation rate increases as temperature increases [71]. On the other hand, low environmental temperature can lead to adaptations such as those observed in psychrophilic and psychrotrophic fungi that survive in Arctic and Antarctic environments; these include but are not limited to, the ability to efficiently store saccharides, the ability to dehydrate and remain dormant [72].

In the presence of salinity stress on pathogens, virulence is either hindered or accelerated. For example, during the infection of powdery mildew fungus, *Oidium neolycopercisi* on tomatoes (*Solanum lycopersicum*), the acumination of Na⁺ and Cl⁻ limits the growth of the pathogen and is subsequently used as a fungal treatment [73]. Contrastingly, an increase in osmotic stress due to high salinity results in accelerated infection in *Setosphaeria turcica* on maize leaves and *Phytophthora parasitica* on tomatoes and citrus roots, causing root rot [74–76].

Drought stress can also cause positive or negative impacts on growth and pathogenicity of microbes. Studies observing mycelium growth of *Phytophthora cinnamomi* and *Phytophthora cambivora* under PEG induced drought stress show that mycelium growth is unaffected by increased osmotic stress [77].

Alternatively, some pathogens are dependent on the availability of water in the surrounding environment for its survival. For example, the quantity of *P. syringae DS3000* present on infected *Arabidopsis thaliana* plant leaves decrease as drought stress increases, therefore, reducing infection to the plant[78].

1.6. bZip transcriptional factors

Transcriptional factors (TFs) are a group of proteins that serve a plethora of functions exclusive to eukaryotes. TFs bind to DNA regions and initiate or regulate the transcription of specific genes by allowing or restricting RNA polymerase to promotor genes [79]. Furthermore, TF's act as switches for gene expression and are categorized into four main types: activators, repressors, enhancers, and silencers. Activators and repressors increase or decrease the expression of genes, while as, enhancers and silencers start or stop the expression of genes.

Basic leucine zipper (bZip) TFs are one of the largest TF class in eukaryotes with diverse structures and biological functions They are involved in development, regulation and stress responses in all eukaryotes, including plants, animals, fungi, and oomycetes[80–84]. bZIPs contain a conserved α -helix consisting of two motifs, the basic region and leucine zipper. The basic region is highly conserved and is approximately 16-18 amino acid residues with an invariant N-x7-R/K domain for nuclear localization and DNA sequence specific binding. The leucine zipper region, is less conserved and is located nine amino acid residues towards the C-terminus [85]. When attached to DNA, the N-terminal attaches to specific sequences while the leucine zipper region mediates homo- and/ heterodimerization producing a superimposed coiled-coil structure[86,87].

Currently, the most well documented bZIPs in oomycetes are from *Phytophthora infestans* and *Phytophthora sojae*. As mentioned in Section 1.1.1, *P. infestans* is the main cause for late blight in potatoes and tomatoes while *P. sojae* is the cause stem and root rot in soybean plants [88–90]. Studies

of bZIPs in *P. infestans* have identified a family of 38 bZIPs encoding genes that show high levels of mRNA expression during mycelium growth, germination of zoospores cysts, sporangia and zoospore formation [91]. In *P. sojae*, the bZIP PsBZP32 has been identified to detect changes to chemicals in surrounding environments, light stress, pathogenicity, oxidative stress regulation and cyst germination [92,93]. Hence, it can be hypothesized that bZIP transcription factors play an important role during developmental and stress adaptation processes in plant pathogens.

1.7. Research questions and hypothesis

Climate change has caused an impact on pathogens and their host interactions, altering growth rates, tolerances, and susceptibility patterns. The main questions being investigated are 1) Does temperature, drought and osmotic stress impact *P. pluvialis* mycelium growth and performance? 2) Are the similarities to bZIP transcriptional factors of *P. pluvialis* to *P. infestans*? 3) Are bZIP transcriptional factors conserved with *Phytophthora* species and in particular between *P. pluvialis* and *P. infestans*? 4) Are expression levels of bZIP transcriptional factors and RxLR effectors altered by abiotic stress? These questions are the foundation for the hypotheses of this research.

1. *P. pluvialis* optimum growth temperature is strain specific.
2. *P. pluvialis* virulence is affected during exposure to salinity and drought stress.
3. *P. pluvialis* mycelium growth is affected during exposure to salinity and drought stress.

1.8. Research purpose

The propose of this thesis is to understand the different variables involved in *P. pluvialis* growth and development. This research aims to understand how external abiotic factors such as salinity and drought stress effects the pathogens growth rate and at a later stage of pathogenicity. Methodically, it will be aimed to design and test primers to quantify transcriptional regulation of an RxLR effector, PpR01

known to be expressed in *P. pluvialis* mycelium and during early infection of pine needles. Furthermore, it is aimed to design and test primers for bZIP transcriptional factors shown to be expressed in mycelium. Lastly, this thesis will aim to understand the genetic conservation between *P. pluvialis* and other *Phytophthora* spp. in particular *Phytophthora infestans* bZIP transcriptional factors and use protein modelling to identify novel domains and motifs.

Chapter 2. : Materials and methods

2.1. Maintenance of *P. pluvialis* on V8 media

P. pluvialis was grown on 10% V8 agar plates (Supplementary table 2), reinoculated every two weeks to maintain growth, prevent starvation and media decay. 10% V8 agar media was prepared, autoclaved, and poured into petri dishes the day before use and cooled thoroughly to prevent condensation and movement of the *P. pluvialis* plug once introduced. Approximately 10 mm plugs were cut out from the old growth plate at the colonies leading edge, using the back end of a large, autoclaved pipette tip, and placed onto the fresh 10% V8 agar plates. The plates were then stored in a dark cupboard at room temperature or in an incubator at 18°C for 7 days before being used for experimentation. This was done for all five strains of *P. pluvialis* used for the experiment: 3000, 3618, 3632, 3880 and 4015. These strains were obtained from Scion, New Zealand and have been cultivated in the University of Canterbury. Alternatively, 10% V8 broth (Supplementary table 2) is used instead of 10% V8 agar when mycelium mats are being prepared for experiments (Section 2.4).

2.2. *P. pluvialis*: Determining optimum growth temperature

Following the method from *Section 2.1*, fresh 10% V8 agar plates were made and *P. pluvialis* strains were grown at the seven different temperatures (four replicates each for temperatures ranging from 15°C to 21°C). Once labelled, the plates were placed into the appropriate incubator and observed for 7

days. Images of mycelium growth were taken on day 1, 3, 5, and 7 using an Epson Perfection V850 Photo scanner at 1,200 pixels.

Temperature		15°C	16°C	17°C	18°C	19°C	20°C	21°C
Strain	3000	4	4	4	4	4	4	4
	3618	4	4	4	4	4	4	4
	3632	4	4	4	4	4	4	4
	3880	4	4	4	4	4	4	4
	4015	4	4	4	4	4	4	4

Table 1: Replicates table for optimal temperature test; *P. pluvialis* strains used and the incubation temperatures each were left at for 7 days. There are 4 replicates for each strain at different temperatures; totalling to 104 plates; 28 per strain or 20 per temperature.

2.3. *P. pluvialis* under salinity and drought stress

Following the method from *Section 2.1* alterations to the 10% V8 agar recipe have been made in form NaCl or PEG addition (Supplementary table 3). *P. pluvialis* plugs were placed onto the altered V8 agar media containing 1 to 5% of NaCl (w/v) and 1 to 5% of PEG (w/v), to induce salinity and drought stress, respectively. The NaCl used was Analytical Reagent grade from LabServ®, while the PEG 3,350 used was from Aldrich®. The plates were placed into an incubator at the newly determined optimum growth temperature, 21°C, for 7 days. Images were taken for mycelial growth on day 1, 3, 5, and 7 using an Epson Perfection V700 Photo scanner at 1,200 pixels. The images of the plates were exported from the Epson Perfection V700 Photo in .TIF format and area of mycelium growth (cm²) was measured with ImageJ using the pixel reference as 400 pixels/cm. R-studio was used to analyze the measured area, perform a two-way ANOVA with a post-hoc Tukey test and produce graphs.

2.4. Abiotic stress effects on mycelium growth for quantitative PCR (qPCR) analysis

As briefly mentioned in *Section 2.1*, due to higher amounts of mycelium needed for applications like qPCR and protein extraction and the advantage of timing of abiotic stress treatment growth of mycelium mats in liquid culture are preferable to mycelium growth on plates. *P. pluvialis* strain 4015 was grown on 10% V8 agar, cut into cubes and placed into an autoclaved sterilized conical flask containing 200mL of 10% V8 broth (Supplementary table 1), ampicillin, and niacin. The flasks were then sealed with a sterilized cotton plug and foil and placed into an incubator with no light for 12 days at 21°C and was manually swirled every few days. Once large mycelium mats were observed they were harvested using aseptic techniques and approximately a dollar-coin-sized amount of mycelial mats were placed into 100 mL of 3% PEG V8 broth, 3% NaCl V8 broth and 10% V8 broth, all containing ampicillin and niacin. The flasks were then placed into an incubator at 21°C for a period of 15 days. Matts were harvested, centrifuged and flash frozen on day 0, 3, 5, 7, 12 and 15.

Concentration		1%	2%	3%	4%	5%
Strain	3000	4	4	4	4	4
	3618	4	4	4	4	4
	3632	4	4	4	4	4
	3880	4	4	4	4	4
	4015	4	4	4	4	4

Table 2: Replicates table for NaCl and PEG treatments; shows the different *P. pluvialis* strains, PEG or NaCl concentrations and the number of replicates used to carry out the experiment. Mycelium growth was measured for each strain with an incubation period of 7 days

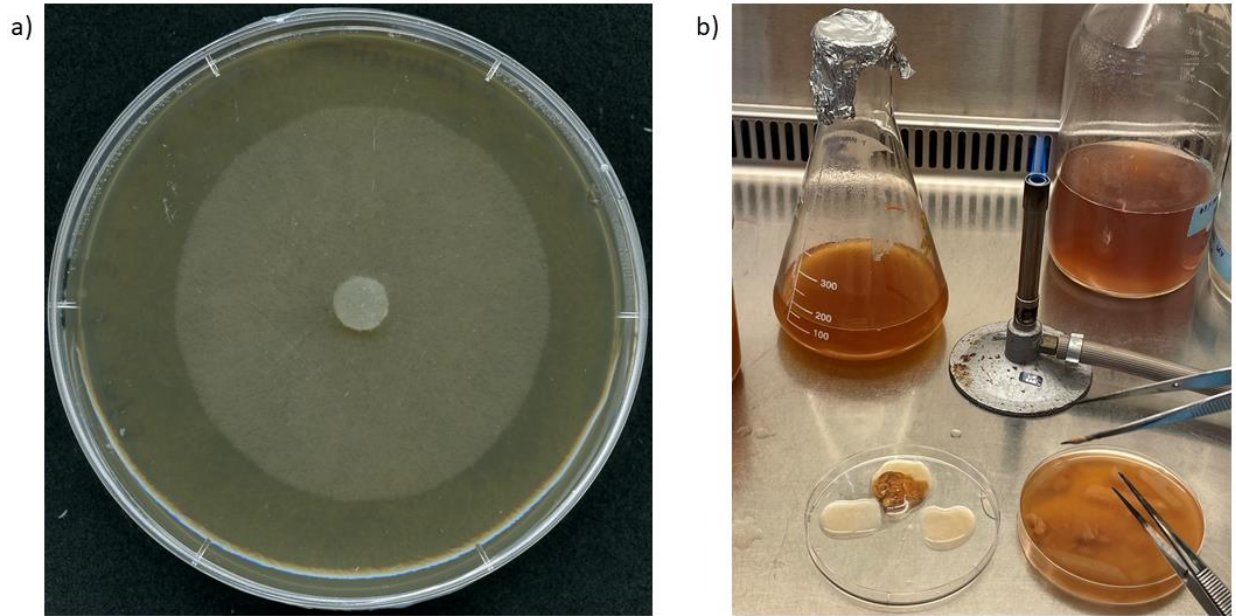


Figure 4: Process of harvesting and growing mycelium in liquid V8 broth; a) *P. pluvialis* strain 4015 grown at 21°C for 7 days. The agar plate was then cut into cubes and placed into sterile conical flasks containing V8 broth.; b) Harvesting process after abiotic stress treatment: Mats were grown for 15 days in 3% NaCl, 3% PEG and V8 broth and manually extracted using sterile tongs, centrifuged, flash frozen and stored at -20°C, to be prepared for qPCR analysis.

2.5. Primer design

Primers were designed using Geneious Prime® 2022.0.1 and further analysed for specificity using NCBI's internal BLAST website. The primers were manufactured by IDT. The criteria for designing primers were as follows: amplicon between 70-100 bp, GC content of 40-60%, no more than 4 repeats, melting temperature of 50-65°C and avoid primers annealing to secondary structures.

2.5.1. *Phytophthora pluvialis* primers for genes of interest

PpR01 primers were made using the nucleotide sequence for the effector, PpR01 [11]. Based on a previous study of *P. infestans* bZIP transcription factor, PITG 04663, expressed during mycelium growth, primers were made for *P. pluvialis* bZIPs [91]. Using NCBI's internal BLAST tool, a tBLASTn was performed of each *P. infestans* bZIP against *P. pluvialis* LC9-1v2 GenBank assembly. The closest

genome sequence match, with the highest e-value, was imported into Geneious Prime® 2022.0.1 the bZIP region and whole protein sequence translated and checked via BLAST on NCBI. Primers were designed for these sequences.

2.5.2. Internal standard primers for *P. pluvialis* actin and COX2

Actin primers were designed for *P. pluvialis*, as an internal standard. Known *Phytophthora infestans* act-A and act-B [94,95] sequences were obtained and a tBLASTn was performed, using IDT's internal BLAST tool, against the *P. pluvialis* LC9-1v2 GenBank assembly. The result with the highest e-value was selected, and an alignment on Geneious Prime® 2022.0.1 was done to determine the actin region in *P. pluvialis* genome. From the now defined actin region, primers were designed for both types of actins to determine match. COX2 primers were also designed as an internal standard for *P. pluvialis*, following the same method mentioned in Section 2.5

2.6. RNA extraction and reverse transcription

RNA extraction was performed following the procedure provided in the Macherey-Nagel™ NucleoSpin™ RNA Plant and Fungi Kit. The RNA extracts were flash frozen and stored at -20°C. To measure the concentrations of RNA extracted the Qubit™ RNA BR Assay Kit was used according to the manufacturer's instructions. The RNA samples were prepared in 1, 1:10 and 1:100 dilutions, and absorbance was measured using the Qubit™ 2 fluorometer and selecting the setting for RNA BR. Dilutions were done due to limitations of the Qubit; the maximum reading is >200 ng/μL and minimum reading of <1 ng/μL. Reverse transcription was performed following the Superscript® VI Reverse transcription by ThermoFisher™. It is assumed that cDNA reverse transcription from RNA is at an efficacy of 100% therefore, cDNA samples were then diluted to 50 ng/μL.

2.7. PCR

2.7.1. Primer reactivity and specificity

A Standard PCR protocol provided by Meridian Bioscience® BIOTAQ™ DNA polymerase was followed to test primers for PpR01, *P. pluvialis* actin, *P. pluvialis* bZIP (PPZIP 07) and COX2 (Supplementary table 4). Conditions for the PCR were, denaturation at 95°C, annealing at 60°C and extension at 72°C (Table 4). To analyse PCR products gel electrophoresis was performed using 1.2% Hyagarose™ LE multipurpose agarose gel in 50mL of 1X TAE (Tris-acetate-ethylene-diamine-tetra acetic-acid) buffer was heated in a microwave for 1 minute following 15 second bursts until fully dissolved, once cooled 2µL of RedSafe™ nucleic-acid staining dye was added. It was then poured into a casting tray with a well comb and allowed to harden for 20 mins before being placed into the gel electrophoresis apparatus. Meridian Bioscience® 100 bp DNA Hyperladder was used as a standard into the first well followed by the PCR products and run for 45 minutes at 100V. Visualisation of the gels were accomplished in ultraviolet light with the G: BOX Chemi-XRQ gel documentation system by Syngene and images captured with the provided software, Genesnap.

Step	Temperature/ °C	Time/ seconds	Cycle
Denaturation	95	30	1
	95	10	35
Annealing	60	15	
Extension	72	10	
Final extension	72	300 (5 mins)	
Hold	10		

Table 3: PCR setting; Meridian Bioscience BIOTAQ™ DNA polymerase

2.8. Reverse transcriptase quantitative PCR (qPCR)

Preparation for quantitative PCR (qPCR) was performed using Thermofisher™ PowerTrack™ SYBR Green Master Mix following the manufacture provided protocol. cDNA used was serially diluted from 1:128 dilution (Table 4). Primers were diluted to 10 μ M from the original stock concentration of 100 μ M (90 μ L of sterile Milli-Q with 10 μ L of stock solution). Table 5 shows the plate map with containing each cDNA dilution for each tube. Quantification of PpR01, *P. pluvialis* actin and *P. pluvialis* bZIP PPZIP 07 were done using two-step qPCR. 10 μ L of the qPCR mixture was pipetted into each qPCR tube with 4 replicates for each dilution. The following conditions were used, Enzyme activation at 95°C for 2 minutes, denaturation at 95°C for 15 seconds and extension at 60°C for 60 seconds (Table 6). qPCR was run on the QIAGEN Rotor-Gene Q using the Rotor-Gene Q Software for analysis. Since the QIAGEN Rotor-Gene Q only has 72 wells, each qPCR run, with separate primers, was performed at separate times. Expression data analysis was performed using Microsoft Excel and heatmaps created using GraphPad Prism (v9.3.1).

cDNA concentration / ng/uL	Dilution factor	Volume of cDNA/ μ L	Nuclease free water/ μ L
50	1	30	-
25	1:2	10 (from stock)	10
12.5	1:4	10 (from 1:2)	10
6.25	1:6	10 (from 1:4)	10
3.125	1:8	10 (from 1:6)	10
1.5625	1:16	10 (from 1:8)	10
0.78125	1:32	10 (from 1:16)	10
0.390625	1:64	10 (from 1:32)	10
0.1953125	1:128	10 (from 1: 128)	10

Table 4: Serial dilution table of cDNA for qPCR; total volume of each concentration is 20 μ L

Primers	PpR01 (10 μ M)				PACT-1 (10 μ M)				BZIP-1 (10 μ M)			
Replicates	1	2	3	4	1	2	3	4	1	2	3	4
	1				1				1:2			
	1:2				1:2				1:4			
	1:4				1:4				1:6			
	1:6				1:6				1:8			
	1:8				1:8				1:16			
	1:16				1:16				1:32			
	1:32				1:32				1:64			
	1:64				1:64				1:128			
	1:128				1:128				1			
	NTC				NTC				NTC			

Table 5: Plate map for qPCR pipetting; PpR01: *P. pluvialis* effector protein primer; PACT-1: *P. pluvialis* actin protein primer; BZIP-1: *P. pluvialis* bZIP protein primer.

Step	Temperature	Time	Cycle
Enzyme activation	95°C	2 minutes	1
Denaturation	95°C	15 seconds	40
Extension	60°C	60 seconds	

Table 6: qPCR settings: Thermofisher™ PowerTrack™ SYBR Green Master for PpR01, PACT-1 and BBZIP-1

2.8.1. Primer efficiency

Primer efficiency was tested using untreated *P. pluvialis* mycelium, strain 4015 and analyzed using the Rotor Gene Q Software to determine CT values, the values were then imported to Microsoft Excel, to determine mean and log concentration. Using this data, a graph and linear regression equation is determined and input into the Thermofisher Science qPCR Efficiency Calculator.

2.9. Phylogenetic analysis

Phylogenetic analysis was used to explore the role similarities and evolutionary conservation of the bZIP transcription factor (TF) family in *P. pluvialis* and *P. infestans*. Protein sequences of already known *P. infestans* bZIP TFs [91] were used to perform BLAST in NCBI's tBLASTn in the *P. pluvialis* isolate LC9-1 genome. The *P. pluvialis* genome sequence with the highest e-value was imported into Geneious Prime® 2022.0.1, the bZIP region, theorized start and stop regions determined and confirmed using INTERPROSCAN and SMART. A BLASTp was then performed on the newly identified *P. pluvialis* bZIP protein sequence to determine common related ancestors, all species from the BLASTp results were selected, omitting repeats, and imported into Geneious Prime® 2022.0.1. Once, imported a MUSCLE alignment was performed on all the protein sequences, which was used to build a Randomized Axelerated Maximum Likelihood (RAxML) tree with a bootstrap setting of 1,000.

All the sequences of both *P. pluvialis* and *P. infestans* bZIP TFs were uploaded to Geneious Prime® 2022.0.1 and a MUSCLE alignment was prepared using the default settings, to build trees from the alignment, the internal Geneious tree building function was used to create an RAxML tree (v8.2.10) and MrBayes (v3.2.6) tree. The settings used for RAxML were GAMMA BLOSUM 62, with a bootstrap setting of 5,000. For the Bayesian tree the rate matrix was set to Poisson and rate variation to gamma distribution. In addition, the trees were uploaded, visualized and protein domains colorized for identification using iTOL (<https://itol.embl.de/>) (v6.5.2).

2.10. Protein modelling

To gain a better understanding of structural conservation and complexity bZIP transcription factor proteins potentially expressed in mycelium were modelled using AlphaFold2 and AlphaFold2-multimer combined with MMseqs2

(<https://colab.research.google.com/github/sokrypton/ColabFold/blob/main/AlphaFold2.ipynb#scrollTo=G4yBrceuFbf3>). Sequence alignments/templates were generated through MMseqs2 and HHsearch [96]. ChimeraX 1.3 was used for visualization of the structural models. The coiled-coil prediction tool waggawagga (<https://waggawagga.motorprotein.de/>) was used for detailed analysis of *P. phuvialis* bZIP14 leucine zipper region.

Chapter 3. Results

3.1. Determining *P. pluvialis* optimum growth temperature

In absence of stress factors, optimum temperature was strain specific. The optimum temperature for optimum mycelial growth for the strains was as follows: For 4015: 20°C, 3880: 18°C, 3632: 21°C, 3618: 16°C and 3000: 17°C (Figure 5). To determine statistical significance a two-way ANOVA was used with the assumption that the growth was dependent on temperature and strain, producing a synergistic effect. The p-value of all the strains is $<2e^{-16}$, which is significant, and indicates that the strain associates with the difference in mycelial growth. The p-value of temperature is insignificant at 0.162 indicating that the change in temperature is not associated with growth rate. The p-value for the interaction between strain and temperature is 0.274, which is insignificant and indicates the relationship between strain and growth rate is independent of temperature (Supplementary Figure 1).

To further interpret interaction, a post hoc Tukey test is performed. The results show all pairwise comparisons between various strains are significant with a p-value of <0.05 , with the exception of 3880-3000 with a p-value of 0.2155041 (Supplementary Figure 2). The temperatures are insignificant with an adjusted p-value of >0.05 (Supplementary Figure 3). Observations can be concluded that growth rate is impacted by strain rather than temperature change.

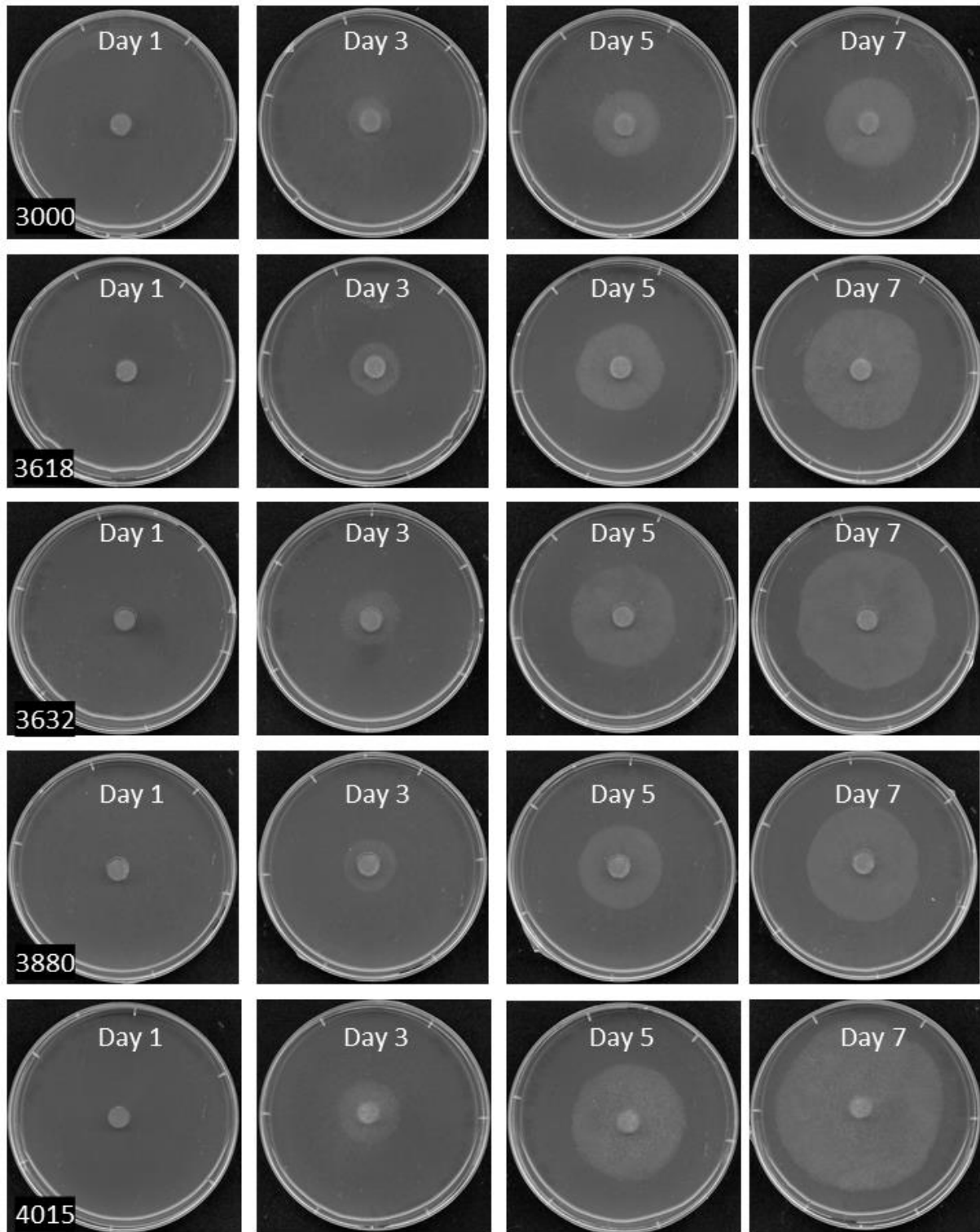


Figure 5: Various strains of *P. pluvialis* grown at temperatures 21°C ; *P. pluvialis* strains 3000, 3618, 3632, 3880 and 4015 grown at 21°C from day 1, 3, 5 and 7. Mycelium growth can be seen growing around the plug.

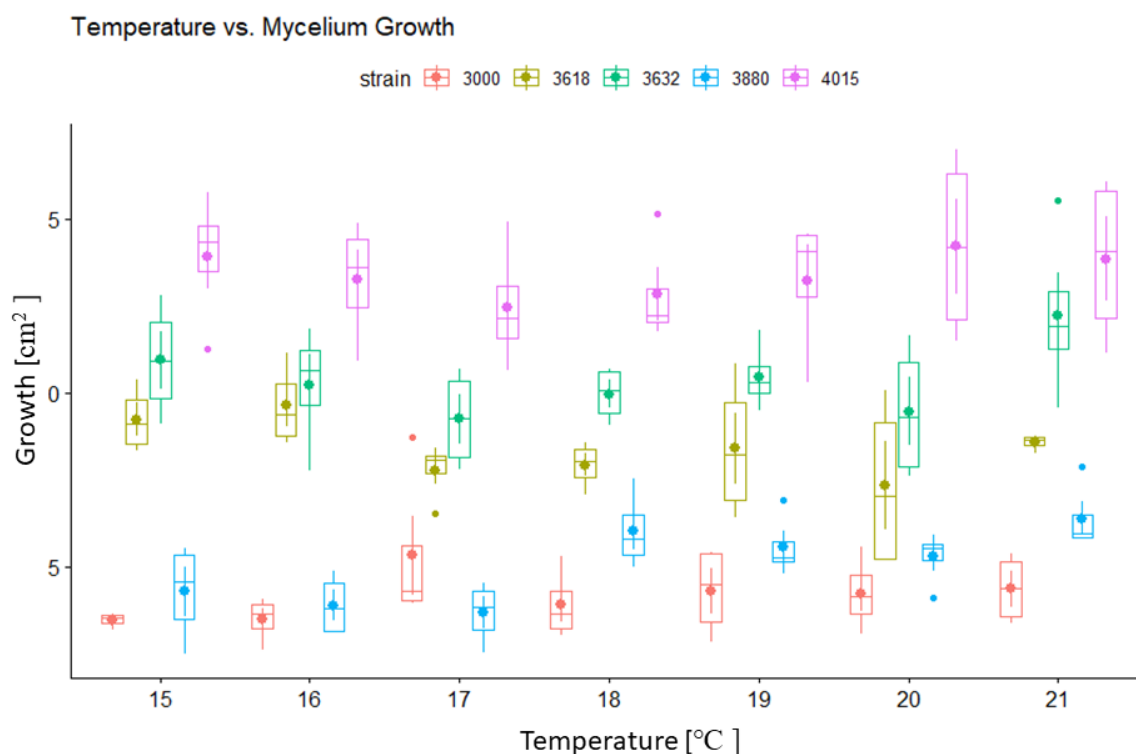


Figure 6: *P. pluvialis* grown at 15°C-21°C; The box- plot shows the average area of mycelium growth during a 7-day growth period. The area of mycelium growth of *P. pluvialis* shows optimum temperature of 4015 is 20°C, 3880 is 18°C, 3632 is 21°C, 3618 is 16°C and 3000 is 17°C; The average temperature is 18.4°C; Biological replicates : 4

3.2. *P. pluvialis* growth rate under abiotic stress

3.2.1. Salinity

Here *P. pluvialis* was grown in the presence of only one stress factor, salinity, at various NaCl concentrations. The growth of mycelium was significantly reduced as the concentration of NaCl in the media increased (Figure7). Statistical conformation was done using two-way ANOVA with the assumption that the growth is dependent on temperature and strain, producing a synergistic effect. The p-value of all the strains is $3.59e^{-07}$, which is significant, and indicates that strain is associated with the difference in mycelial growth. The p-value of concentration is significant at $<2e^{-16}$, indicating that the

change in concentration is associated with growth rate. The p-value for the interaction between strain and concentration is $7.64e^{-07}$, which is significant and indicates the relationship between strain and mycelial growth is dependent on the change in concentration of NaCl (Supplementary Figure 4).

To further interpret interaction between strain and concentration, a post hoc Tukey test is performed. The results show all pairwise comparisons between various concentration are significant with an adjusted p-value of <0.05 , with an exception for the 4% and 5% of NaCl pair being insignificant at 0.9801505 (Supplementary Figure 5). For the comparison of different strains, the p-value is <0.05 , with the exception of the strains, 3632-3000, 4015-3000, 3632-3618, 4015-3618 and 4015-3880 showing p-values >0.05 , therefore being insignificant (Supplementary Figure 6). This data determines that the growth rate is dependent of strain and concentration ($p<0.05$). Therefore, concluding that the growth rate is impacted by strain and concentration change.

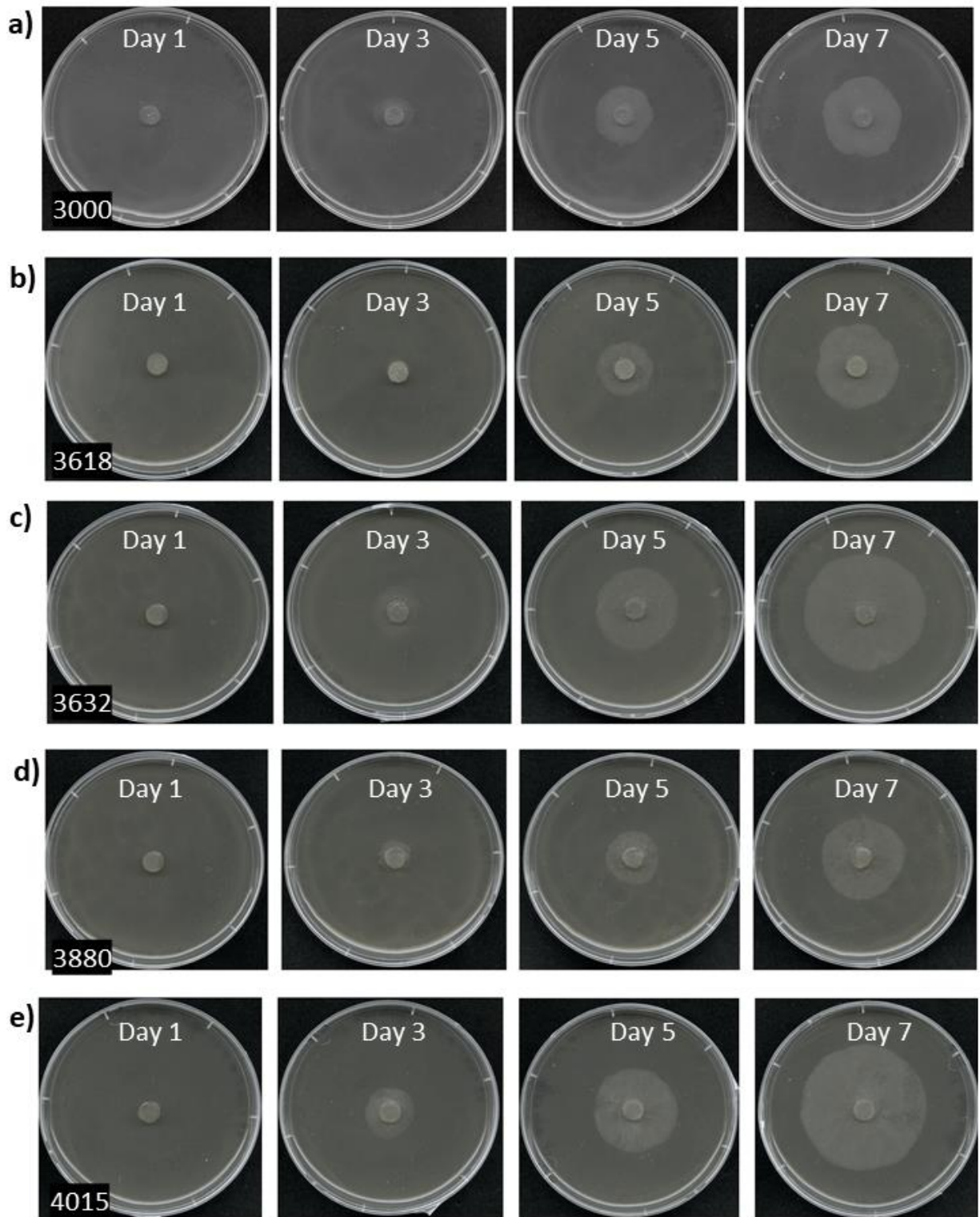


Figure 7: *P. pluvialis* grown on V8 media under salinity stress: *P. pluvialis* strain 4015 grown on V8 agar containing 5% NaCl in media, grown at 21°C for 1-7 days. No mycelium growth is observed.

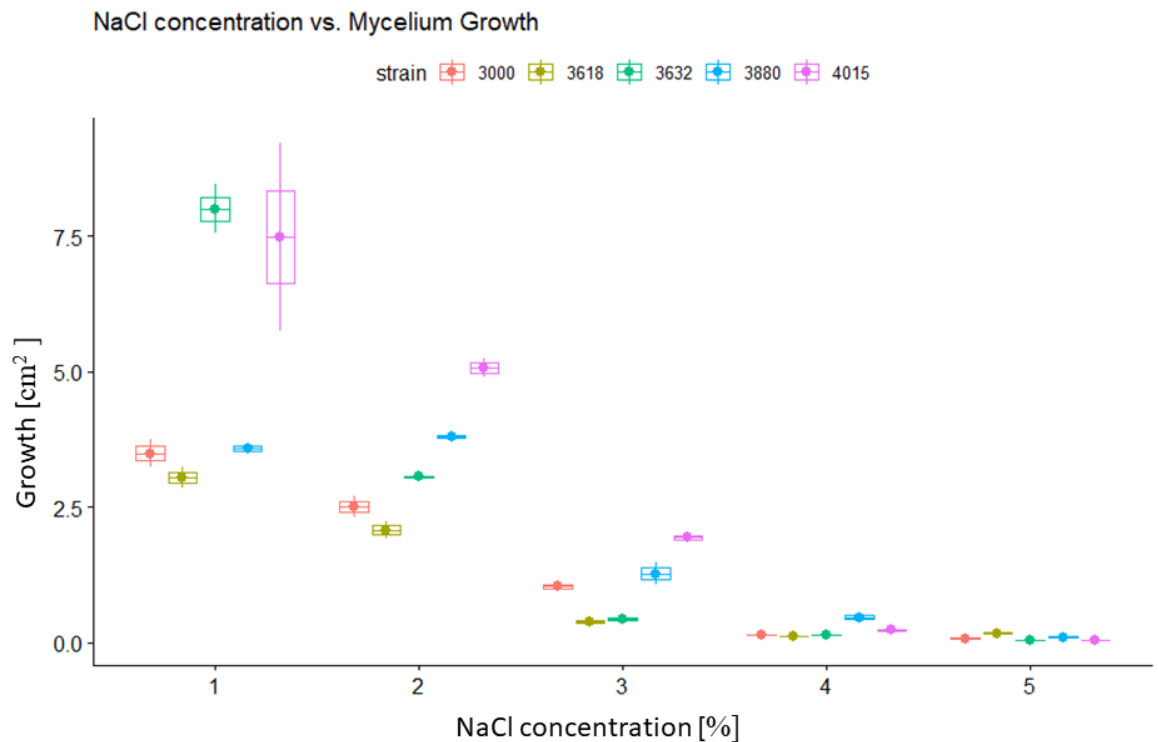


Figure 8: Analysis of *P. pluvialis* under salinity stress; The box- plot shows the average area of mycelium growth during a 7-day growth period. The area of mycelium growth of *P. pluvialis* under salinity stress declines, as the concentration of NaCl increases. The decline of growth is independent of strain and is observed in all strains.; *P. pluvialis* strains; Pink: 4015, Blue: 3880, Green: 3632, Yellow: 3618, Red: 3000; Biological replicates: 4

3.2.2. Drought

Drought stress was induced at various concentrations of PEG on *P. pluvialis* . Interestingly, mycelium growth had did not change significantly with increasing concentration of PEG (Figure 9). Statistical conformation was done using two-way ANOVA with the assumption that the growth is dependent on PEG concentration and strain, producing a synergistic effect. The p-value of all the strains is $<2e^{-16}$, which is significant, and indicates that the strain is associated with the difference in mycelial growth. The p-value of concentration is significant at 0.0315, indicating that the change in concentration of PEG is associated with growth rate. The p-value for the interaction between strain and concentration is $5.19e^{-}$

⁰⁶, which is significant and indicates the relationship between concentration and mycelial growth is dependent on the strain (Supplementary Figure 7).

Further interpretation of interaction between strain and concentration of PEG, a post hoc Tukey test was performed, which shows all pairwise comparisons between various concentration are insignificant with an adjusted p-value of >0.05 (Supplementary Figure 8). For the different strains, all pairwise comparisons are significant with the p-values being <0.05 (Supplementary Figure 9). This data determines that the growth rate is dependant of strain and concentration ($p<0.05$). Therefore, concluding that the growth rate is impacted by strain and concentration change.

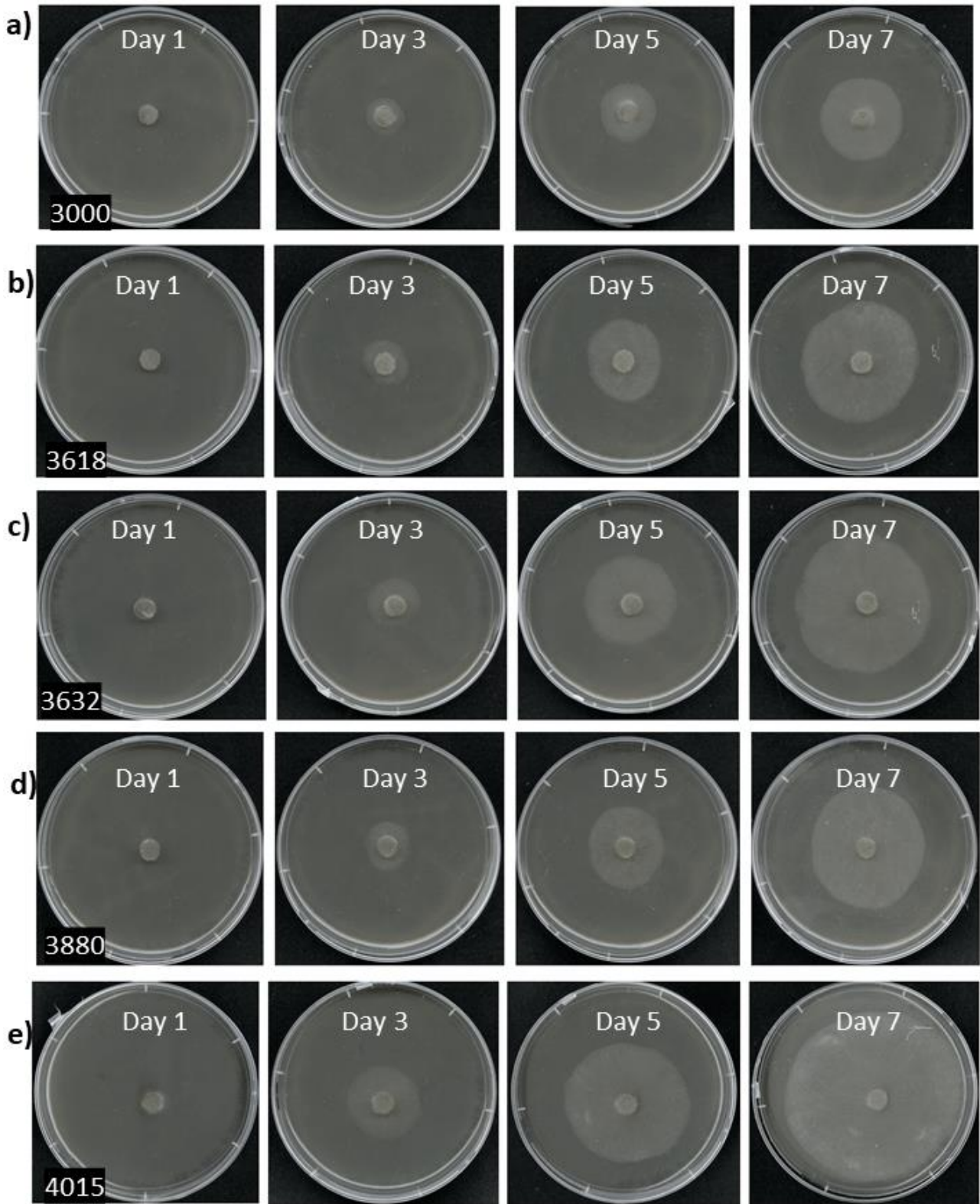


Figure 9: *P. pluvialis* grown on V8 agar media under drought stress; *P. pluvialis* strain 4015 grown on V8 agar containing 5% PEG (polyethylene glycol), grown at 21°C for 1-7 days. Mycelium growth seen around the plug. Brightness and contrast adjusted to 20% to be able to visualise mycelium growth clearly.

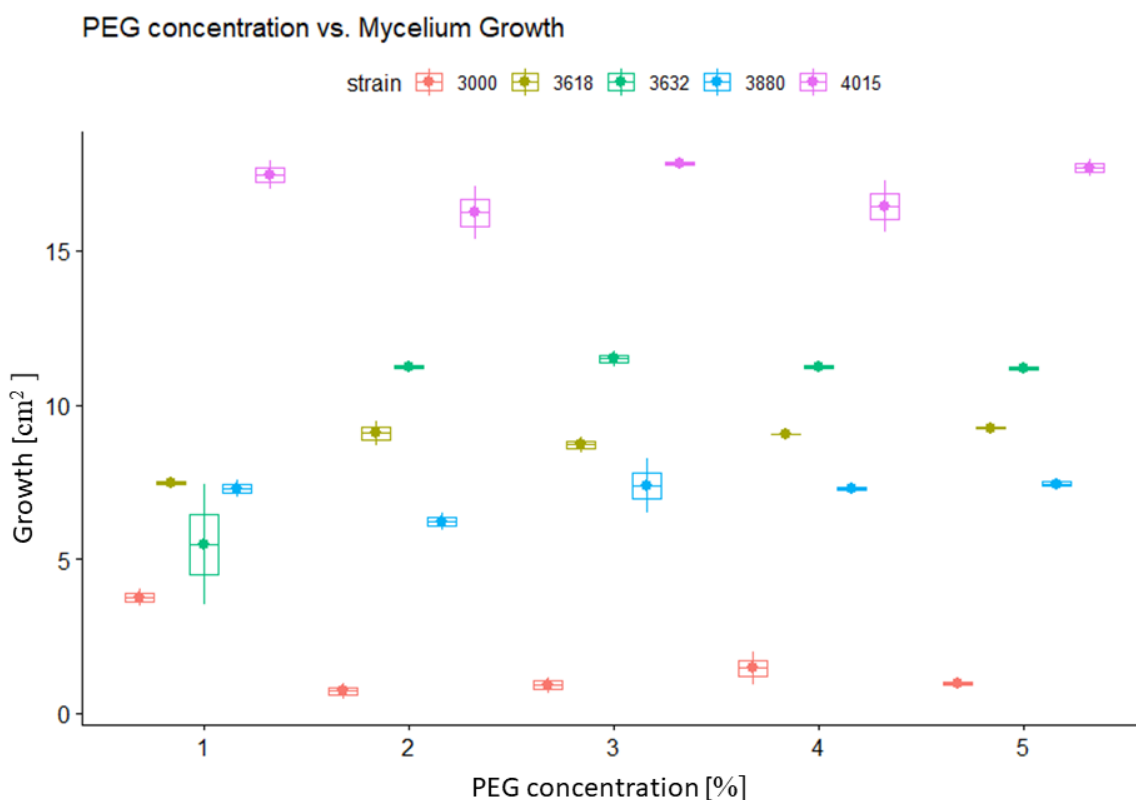


Figure 10 :Analysis of *P. pluvialis* under drought stress; The box- plot shows the average area of mycelium growth during a 7-day growth period. The area of mycelium growth of *P. pluvialis* under drought stress remains constant, as the concentration of polyethylene glycol (PEG) increases. The growth pattern is strain specific, 4015, 3880 and 3618 have no changes in growth.; *P. pluvialis* strains; Pink: 4015, Blue: 3880, Green: 3632, Yellow: 3618, Red: 3000; Biological replicates: 4

3.3. Primers and PCR

Primer pairs for *P. pluvialis* effector protein (PpR01), *P. pluvialis* actin (PACT) and *P. pluvialis* bZIP transcriptional factor (BZIP) to be tested were made using Geneious Prime® 2022.0.1 (Supplementary table 4). The primers were confirmed by PCR and gel electrophoresis and denotes the expression of PpR01, actin and bZip TFs in *P. pluvialis* mycelium (Figure 11). Table 8 shows the expected product sizes derived from Geneious Prime® 2022.0.1 and the obtained product size for PPR01-1, which shows bands for all primers were expected at 100-200bp, PACT-1 a band at 120-180 bp and BZIP-1 a prominent band at 150-190 bp with the presence of multiple bands above 100 bps.

Primer identifier	Forward sequence (5'-3')	Reverse sequence (3'-5')
PPR01-1	AAGCATTCCCCGTATCACG	TCTTCGTCGTCCTTGGCATC
PACT-1	CGACCTGCGCCTTAGTGAAA	GCCCATTTTCGTCGGTTTGAG
BZIP-1	ATCTCAGCGTGGATGGAAGC	TGTTTTCCAGCGTCCTCCTC

Table 7: Primer chosen from gel electrophoresis; PPR01-1: *Phytophthora pluvialis* effector protein primer; PACT-1: *P. pluvialis* actin protein primer; BZIP-1: bZip transcriptional factor protein primer

Primers	Expected product size/ bp	Obtained product size/ bp
PpR01-1	131	100-200
PACT-1	100	120-180
BZIP-1	100	150-190

Table 8: Selected primers and their base pair lengths; PpR01-1, PACT-1 and BZIP-1 selected, and their Geneious Prime® 2022.0.1 base pair lengths compared to experimentally determined gel electrophoresis base pair lengths



Figure 11: Gel electrophoresis of primers tested for PpR01, *P. pluvialis* actin and *P. pluvialis* BZIP TF; a) 100 bp Hyperladder from Bioline; b) PpR01 primers tested, PpR01-1 and PpR01-2 shows transcription at approximately 100 base pairs, PpR03, PpR04 and COX2 are undetected .; c) bZip primers tested; BZIP-1 and PACT-1 show transcription at >100 and <200 base pairs, BZIP2 forms primer dimer and BZIP3 and BZIP4 show no bands.

3.4. RNA and cDNA preparation

To confirm the Qubit Fluorometer 2 readings, a nanodrop reading on cDNA after reverse transcription was performed (Table 9). cDNA diluted to 50 ng/ μ L using Qubit derived concentrations (Table 10).

Sample	Day	Nanodrop/ [ng/ μ L]	Qubit/ [ng/ μ L]
V8	0	724	574
V8	3	138.3	110
V8	5	371	140
V8	7	230.3	214
V8	12	515.1	245
NaCl	3	14.2	12.1
NaCl	5	23.3	11
NaCl	7	226.4	206
NaCl	12	237.4	74
PEG	3	342.9	340
PEG	5	592.1	406
PEG	7	590.7	124
PEG	12	800.5	622

Table 9: RNA concentrations from Nanodrop and Qubit Fluorometer 2; RNA extracted from *P. pluvialis* mycelium grown at 0, 3, 5, 7 and 12 days; V8: mycelium grown in V8 broth, NaCl: mycelium grown in 3% NaCl V8 broth, PEG: mycelium grown in 3% PEG V8 broth.

Sample/ Day	Original cDNA concentration / ng/uL	cDNA/ μ L	Sterile Milli-Q/ μ L	Final cDNA concentration/ ng/uL
V8-0	724	1.74	18.26	50
V8-3	138.3	9.09	10.91	
V8-5	371	7.14	12.86	
V8-7	230.3	4.67	15.33	
V8-12	515.1	4.08	15.33	
NaCl-3	14.2*			
NaCl-5	23.3*			
NaCl-7	226.4	4.85	15.15	
NaCl-12	237.4	13.5	6.5	
PEG-3	342.9	2.94	17.06	
PEG-5	592.1	2.46	17.54	
PEG-7	590.7	8.06	11.94	
PEG-12	800.5	1.06	18.94	

Table 10 : cDNA dilution table; shows dilution of *P. pluvialis* mycelium cDNA dilution to 50 ng/uL in 20uL; “*”: concentrations too low so no dilution was performed.

3.5. Reverse transcription quantitative PCR

3.5.1. PpR01 primer binding efficiency in *P. pluvialis* mycelium samples

qPCR was performed on mycelium samples of *P. pluvialis* strain 4015. CT values for the transcript of the RxLR effector PpR01 were obtained from the Rotor-Gene Q Series Software after qPCR of untreated *P. pluvialis* mycelium. CT values were imported into Microsoft Excel to produce a standard curve and a linear regression equation for PpR01 primers. The linear regression equation was $y = -5.0255x + 23.828$ with an R^2 value of 0.9152, (Figure 12A), this shows a PCR efficiency of 1.58119406519 and therefore a PCR efficiency percentage of percentage of 58.12%. From the Rotor-

Gene Q Series Software, the linear regression equation automatically produced was $y = -4.626x + 32.096$ with an R^2 value of 0.83705 (Figure 12B). The PCR efficiency was 0.65, therefore the PCR efficiency percentage is 64.50%.

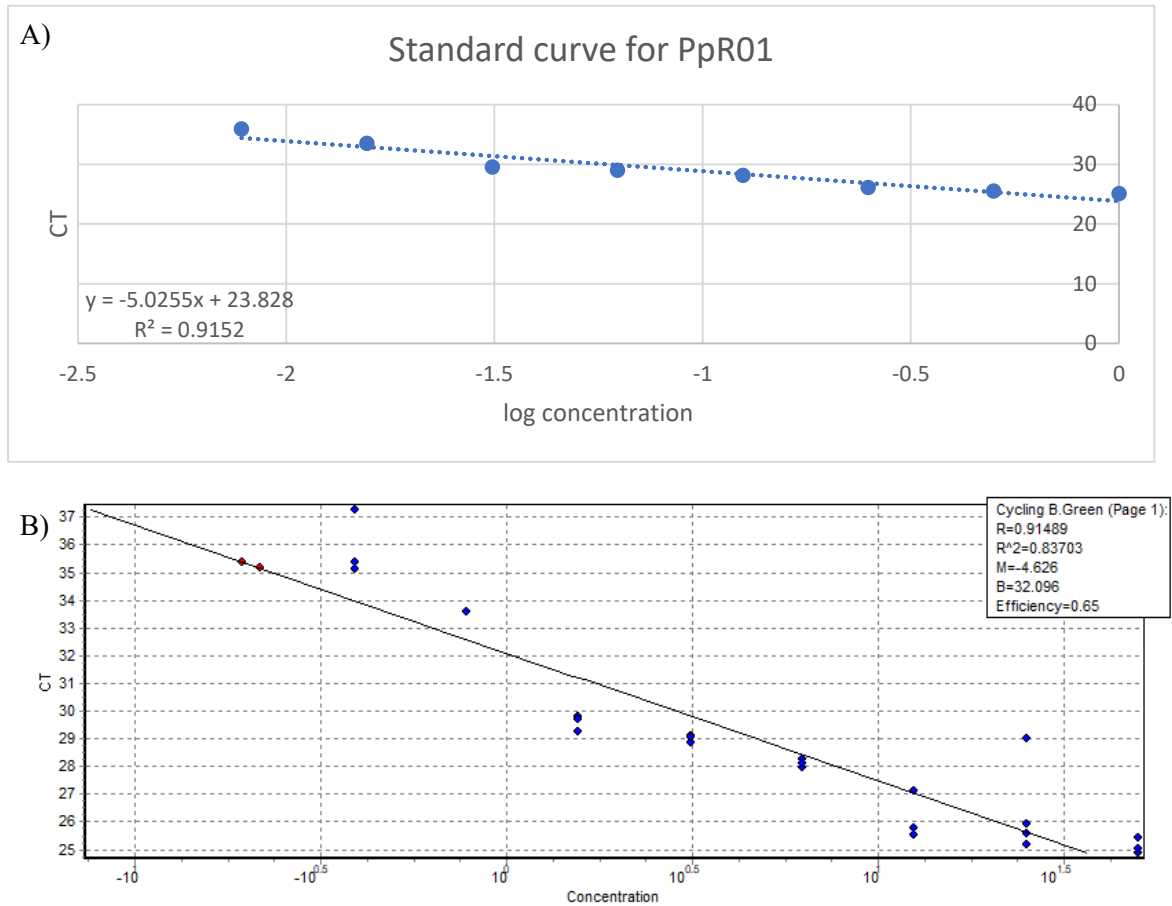


Figure 12: Standard curve of PpR01; A) Standard curve made in Microsoft Excel B) Standard curve exported from Rotor Gene-Q Software; Dilution factor : 2 fold; Number of replicates for each dilution was 4; Biological replicates: 4

3.5.2. Actin efficiency

PACT-1 actin expression, CT values were obtained from the Rotor-Gene Q Series Software after qPCR. The CT values were imported into Microsoft Excel to produce a standard curve and a linear regression equation for PACT-1. The linear regression equation was $-5.4432x + 26.566$ with an R^2 value of 0.8946 (Figure 13A), this shows a PCR efficiency of 1.526566 and therefore a PCR efficiency percentage of 52.66% for mycelial samples. From the Rotor-Gene Q Series Software, the linear regression equation automatically produced was $y = -4.971x + 35.127$ with an R^2 value of 0.68952. The PCR efficiency was 0.59, therefore the PCR efficiency percentage is 58.92% (Figure 13B). Overall, PACT-1 is relatively low expressed in mycelial samples.

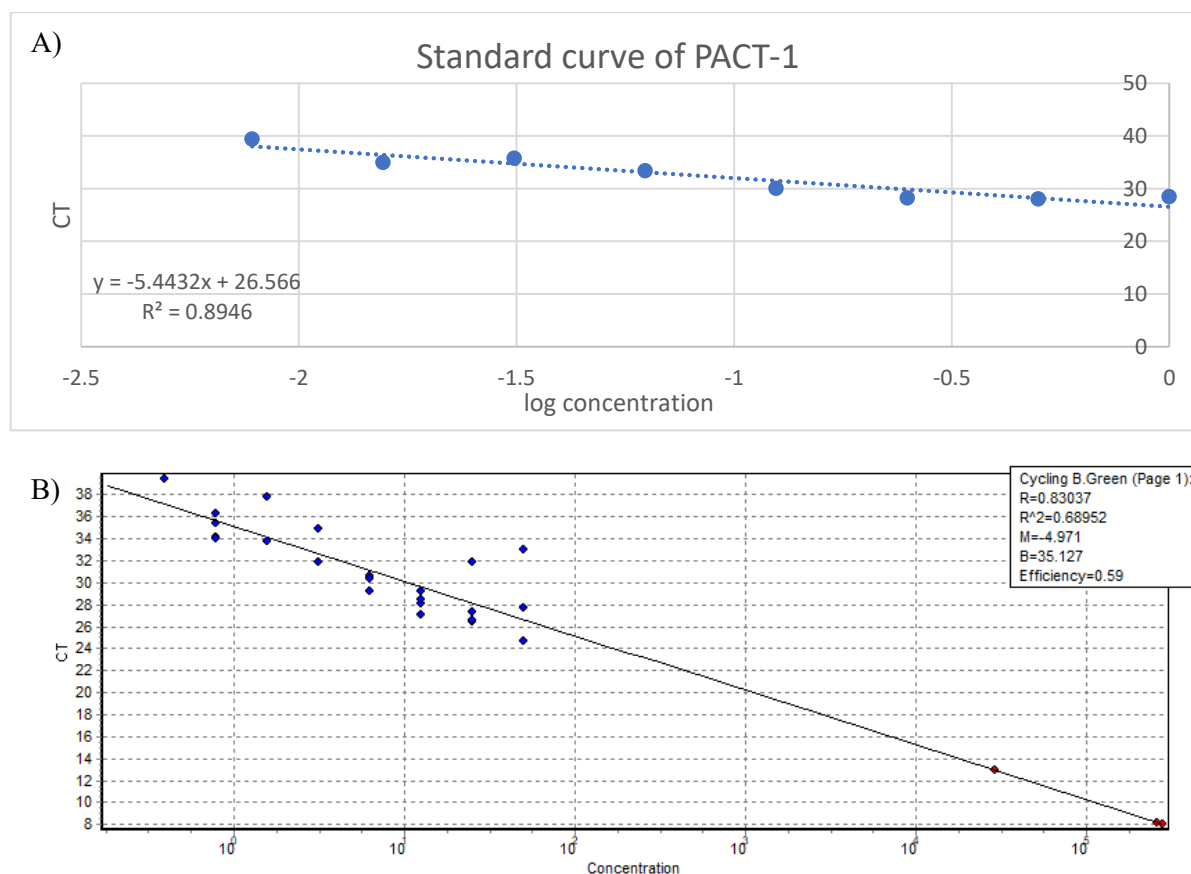


Figure 13: Standard curve of PACT-1; A) Standard curve made in Microsoft Excel B) Standard curve exported from Rotor Gene-Q Software; Dilution factor : 2 fold; Number of replicates for each dilution:

4

3.5.3. Expression of PpR01 under salinity and drought stress

Pathogenicity was evaluated by the expression of *P. pluvialis*, strain 4015, RxLR effector PpR01, during abiotic stress treatments. Normalization was done using actin as a reference gene. cDNA was extracted from *P. pluvialis* mycelium mats undergoing no treatment, NaCl treatment and PEG treatment for day 0, 3, 5, 7 and 12. Figure 14 shows a graph and heat map of the expression of PpR01 during NaCl induced salinity stress and PEG induced drought stress.

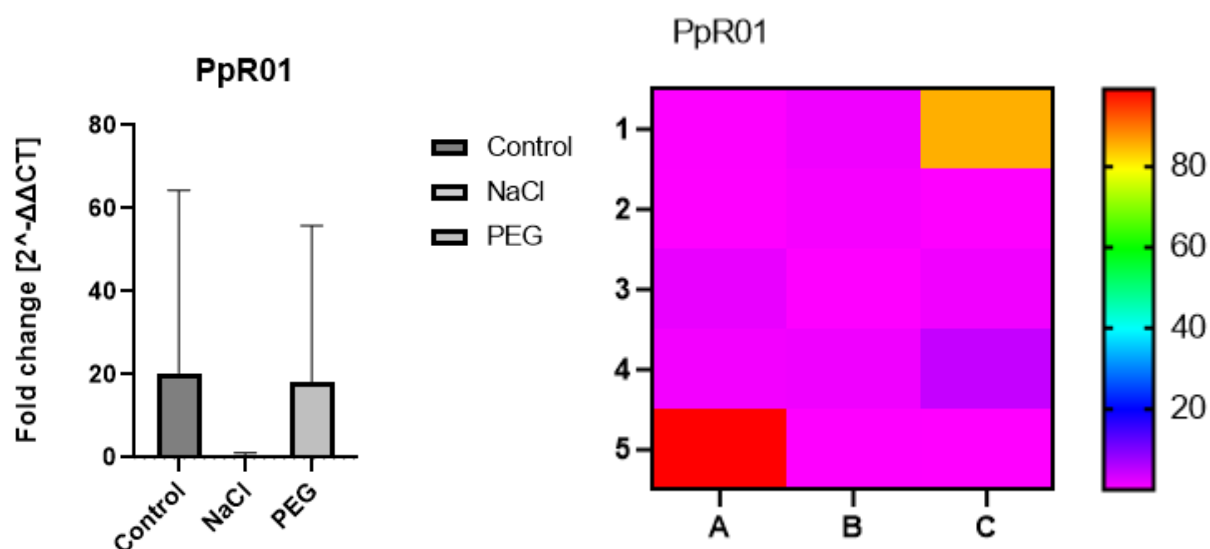


Figure 14: Expression of PpR01 during salinity and drought stress induced by NaCl and PEG, respectively. The heat map shows the expression of PpR01 during no treatment, 3% NaCl treatment and 3% PEG treatment; Expression of PpR01 is seen during no treatment and PEG treatment and is not expressed during NaCl treatment; A: control, B: NaCl and C: PEG

3.5.4. Expression of bZIP, PPZIP 07, under salinity and drought stress

The effects of mycelium growth were determined by determining the expression of bZIP transcription factor, PPZIP 07 during abiotic stress treatments. Normalization was done using actin as a reference gene. cDNA was extracted from *P. pluvialis* mycelium mats undergoing no treatment, NaCl treatment and PEG treatment for day 0, 3, 5, 7 and 12-day. Figure 15 shows a heat map with the expression of PPZIP 07, responsible for mycelium growth. Therefore, mycelium growth does not occur during salinity stress, though occurs during drought stress.

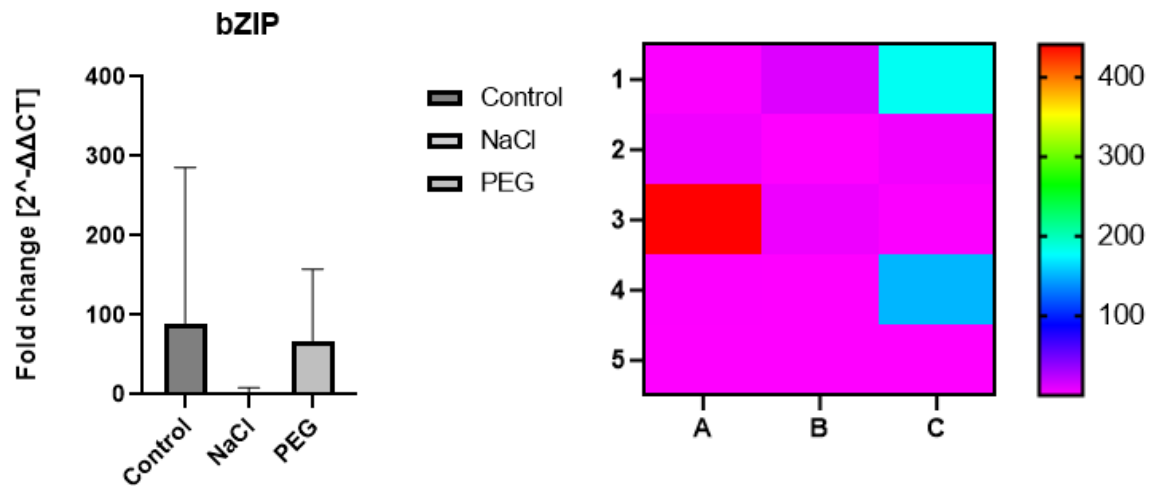


Figure 15: Expression of PPZIP 07 during salinity and drought stress induced by NaCl and PEG, respectively. The graph and heat map both show the expression of bZIPs during no treatment, NaCl treatment and PEG treatment; Expression of bZIP is seen during no treatment and PEG treatment and is not expressed during NaCl treatment; A: control, B: NaCl and C: PEG

3.6. Phylogenetic analysis

3.6.1. Conserved *P. pluvialis* and *P. infestans* bZIP transcription factors

Known *P. infestans* bZIP regions, were used to predict and determine *P. pluvialis* bZIP regions on its genome sequence using NCBI's tBLASTn and Geneious Prime. The BLAST and MUSCLE alignment of all known *P. infestans* bZIPs and newly found *P. pluvialis* bZIP regions revealed that multiple *P. infestans* bZIPs were identified on the same *P. pluvialis* bZIP sequence. The results of a tBLASTn performed on *P. infestans* bZIP, PITG 07437, PITG 07438, PITG 07440 and PITG 07449, revealed that for all four bZIPs, the result was same *P. pluvialis* bZIP sequence on the same genome sequence. Therefore, the *P. pluvialis* bZIP name derived from all four *P. infestans* bZIPs, is PPZIP_09. This is also highlighted and seen for PPZIP 11, PPZIP 12 and PPZIP 14 (Table 11) .

<i>P. infestans</i> bZIP	<i>P. pluvialis</i> bZIP	<i>P. pluvialis</i> genome accession number
PITG_00964	PPZIP_01	LGTU01000417.1
PITG_02328	PPZIP_02	LGTU01000136.1
PITG_02329	PPZIP_03	LGTU01000136.1
PITG_02733	PPZIP_04	LGTU01000177.1
PITG_03223	PPZIP_05	LGTU01000640.1
PITG_04228	PPZIP_06	LGTU01000658.1
PITG_04663	PPZIP_07	LGTU01000025.1
PITG_04908	PPZIP_08	LGTU01000388.1
PITG_07437	PPZIP_09	LGTU01002844.1
PITG_07438	PPZIP_09	LGTU01002844.1
PITG_07440	PPZIP_09	LGTU01002844.1
PITG_07449	PPZIP_09	LGTU01002844.1
PITG_08159	PPZIP_10	LGTU01000180.1
PITG_09190	PPZIP_11	LGTU01000164.1
PITG_09198	PPZIP_11	LGTU01000164.1
PITG_09199	PPZIP_11	LGTU01000164.1
PITG_09200	PPZIP_11	LGTU01000164.1
PITG_09201	PPZIP_11	LGTU01000164.1
PITG_09279	PPZIP_12	LGTU01000709.1
PITG_09280	PPZIP_12	LGTU01000709.1
PITG_09816	PPZIP_13	LGTU01000265.1
PITG_10557	PPZIP_14	LGTU01000381.1
PITG_10558	PPZIP_14	LGTU01000381.1
PITG_10798	PPZIP_15	LGTU01000987.1
PITG_11664	PPZIP_16	LGTU01000164.1
PITG_11668	PPZIP_17	LGTU01000164.1
PITG_11671	PPZIP_18	LGTU01000164.1
PITG_13196	PPZIP_19	LGTU01001895.1
PITG_13521	PPZIP_20	LGTU01001687.1
PITG_13587	PPZIP_21	KQ473662.1
PITG_15136	PPZIP_22	LGTU01000703.1
PITG_15584	PPZIP_23	LGTU01000853.1
PITG_16038	PPZIP_24	LGTU01000052.1
PITG_16183	PPZIP_25	LGTU01000628.1
PITG_17483	PPZIP_26	LGTU01001144.1
PITG_17706	PPZIP_27	LGTU01000325.1
PITG_18417	PPZIP_28	LGTU01000263.1
PiBZP1	PPZIP_29	LGTU01000164.1

Table 11: *P. infestans* bZIP with renamed *P. pluvialis* bZIP; *P. infestans* sequences were obtained from: Yang, X., Tyler, B.M.://doi.org/10.5598/ima fungus.2017.08.02.09 and used to identify corresponding *P. pluvialis* bZIP sequences.; *P. infestans* bZIP sequence names and new *P. pluvialis* bZIP sequence names (Green). The *P. pluvialis* accession number shows the sequence in which the bZIP was identified in.; Primers for bZIP expression analysis were made from PPZIP_07 (yellow).

3.6.2. Phylogenetic similarities

3.6.2.1. bZIP family conservation of *P. pluvialis* and *P. infestans*

To determine the relationship and similarity between *P. pluvialis* and *P. infestans* bZips, a RAxML tree was produced from the aligned sequences in Section 3.6.1, using Geneious Prime. The branches of the RAxML tree displays the bootstrap percentage value >75%, these values and the tree correspond with Table 11 in Section 3.6.1., with the exception of, the clades highlighted on Figure 17

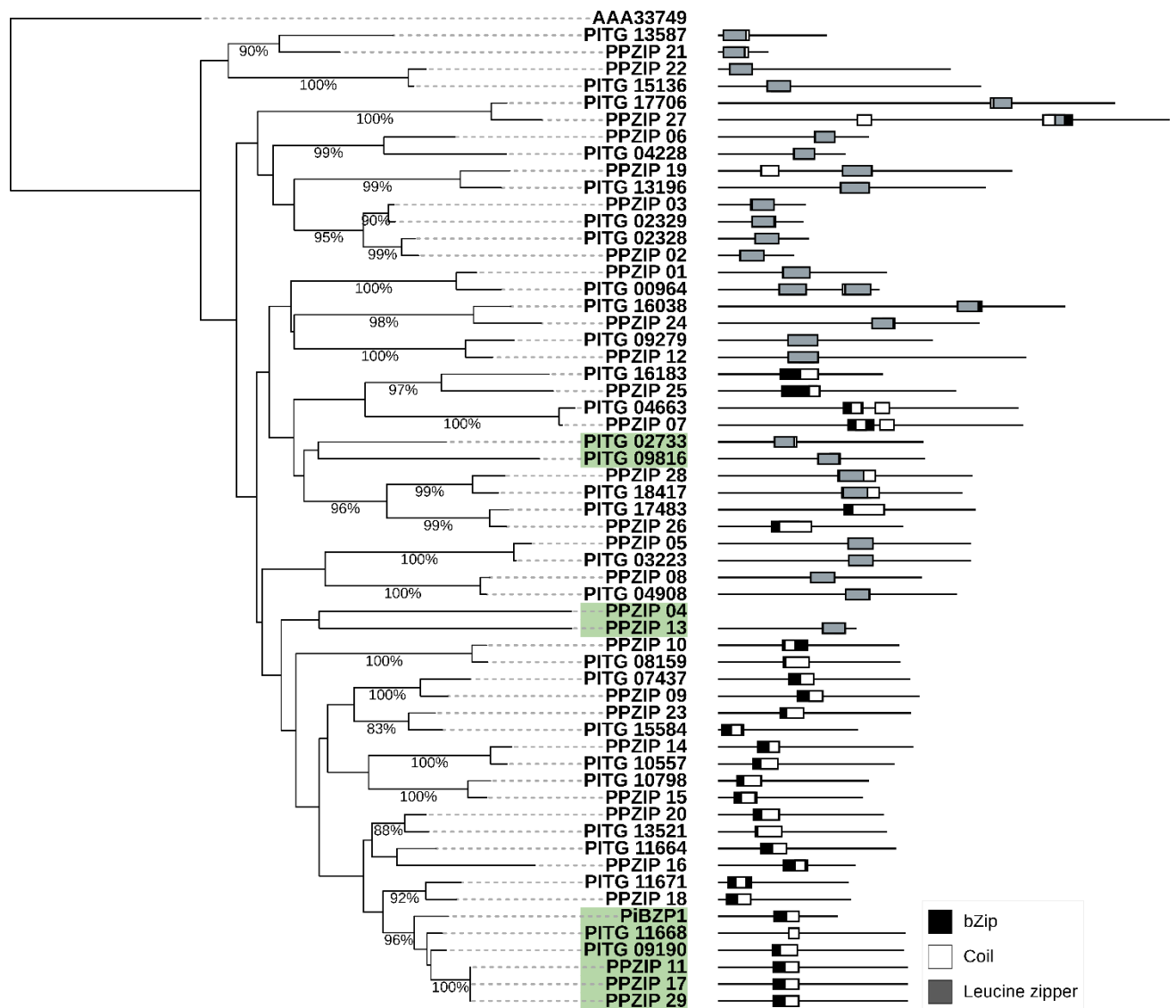


Figure 16: RAxML tree of *P. pluvialis* and *P. infestans* bZIPs. On the branches are the bootstrap values, values < 75% were removed from the tree; Discrepancies between *P. infestans* and *P. pluvialis* bZIP families when compared to Table 11 (Green); The right-hand side shows the position of bZIP, coiled-coil structure and leucine zipper along the length of the protein sequence. Black: bZip, White: Coil, Grey: Leucine zipper

3.6.2.2. bZIP family in *P. pluvialis* and closely related ancestors

A BLASTp using NCBI's BLAST tool, was performed on the newly identified *P. pluvialis* bZIPs against all organisms. The top results, with the highest e-values, for *P. pluvialis* bZIP, PPZIP 14 identified were *Phytophthora* spp., specifically *Phytophthora pseudosyringae*, which is also part of clade 3 in the *Phytophthora* family tree (Figure 2). Supplementary Figure 10 also show the relationship between *P. pluvialis* and *P. pseudosyringae* for PPZIP 1, PPZIP 2, PPZIP 3 and PPZIP 4. These relationships were confirmed using a RAxML phylogenetic tree (Figure 16)

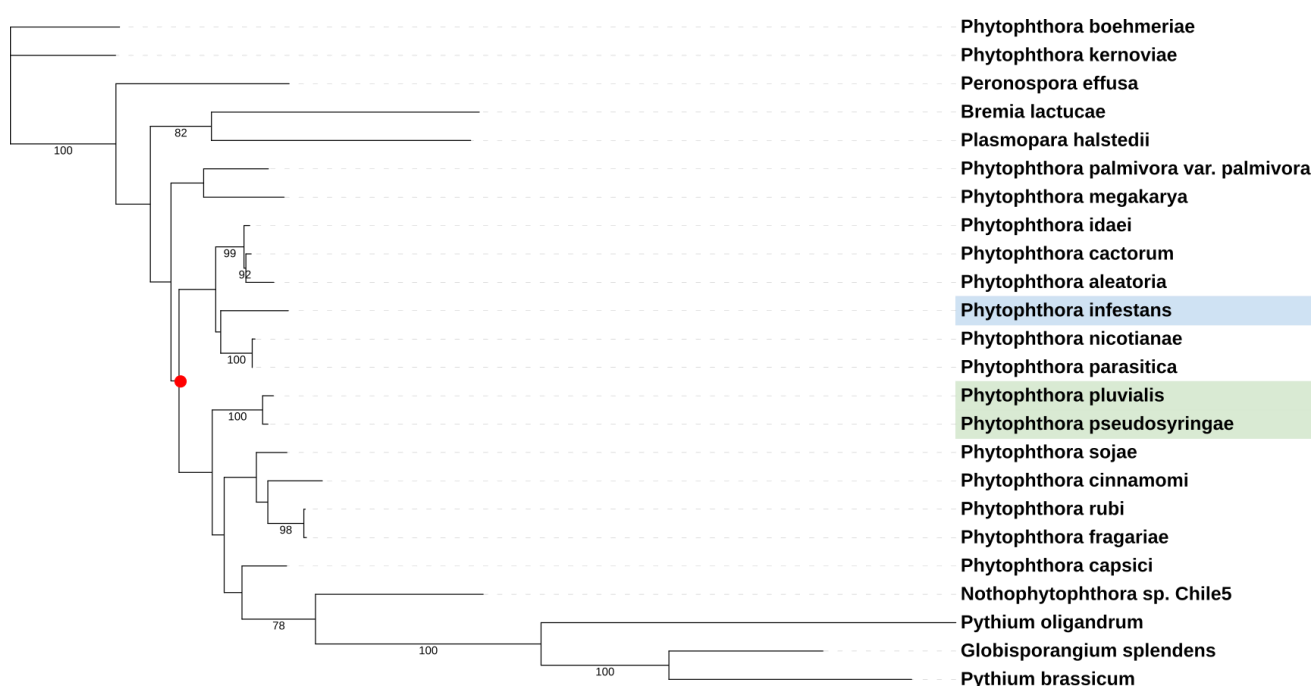


Figure 17: Analysis of PPZIP 14 shows the bootstrap values of *P. pluvialis* and *P. pseudosyringae* being 100%. The red node shows the most recent common ancestor of *P. pluvialis* and *P. infestans*.

3.7. Protein models

In the following *P. pluvialis* protein sequences of PPZIP 10, 13 17 and 24 were used for protein modelling by AlphaFold2. All proteins are potentially expressed during various stages of the oomycete life cycle (Figure 2A) and will be further studied in the future. Structural models confirmed that it is

likely that the four proteins form dimers to interact with the DNA and contain different length of Leucine zipper domains and DNA interaction domains (indicated in blue, Figure. 18). Additionally, all proteins contained a head group involved in formation of dimers with further potential regulatory and protein-protein interaction function. Interestingly, all four analysed proteins contained a central beta sheet in the head group of the ZIP protein. A more detailed analysis was accomplished for PPZIP14 which contains a classical Leucine zipper domain (Figure 19), consisting of an $Lx_6Lx_6Lx_9$. The Leucine zipper domain is followed by the basic region involved in DNA binding. The helical wheel view shows that Leucine's in position a, d and a', d' of the dimers form hydrophobic interactions and amino acids in position e, g and e', g' form polar interactions, which stabilizes the L.

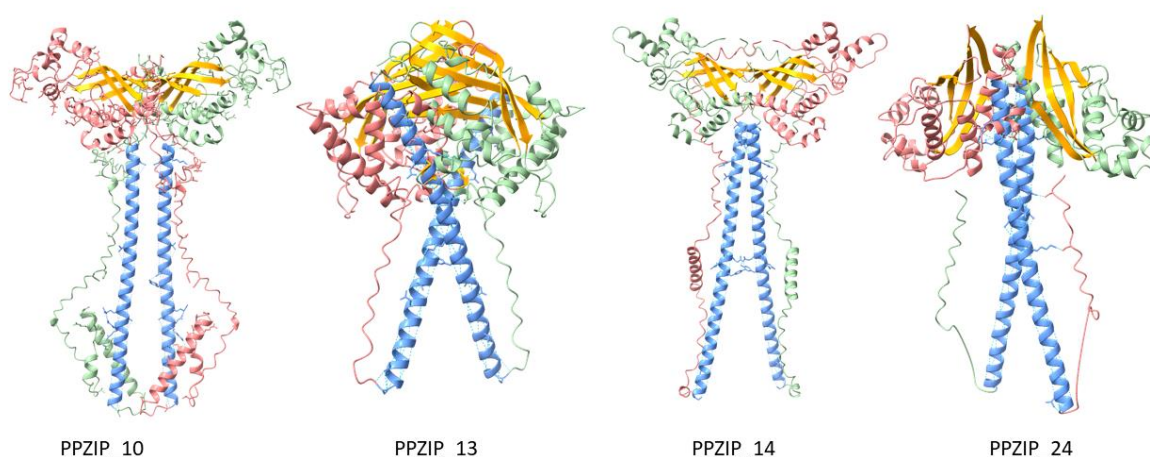


Figure 18: Protein models of *P. pluvialis* bZIP transcription factor homodimers by AlphaFold2. The leucine zipper and DNA binding domain is shown in blue, the protein part not involved in the DNA binding domain are indicated in green (monomer A1) and pink (monomer A2). Modelling has indicated that this class of leucine zippers contains a central beta-sheet (yellow) in the head group of the transcription factor.

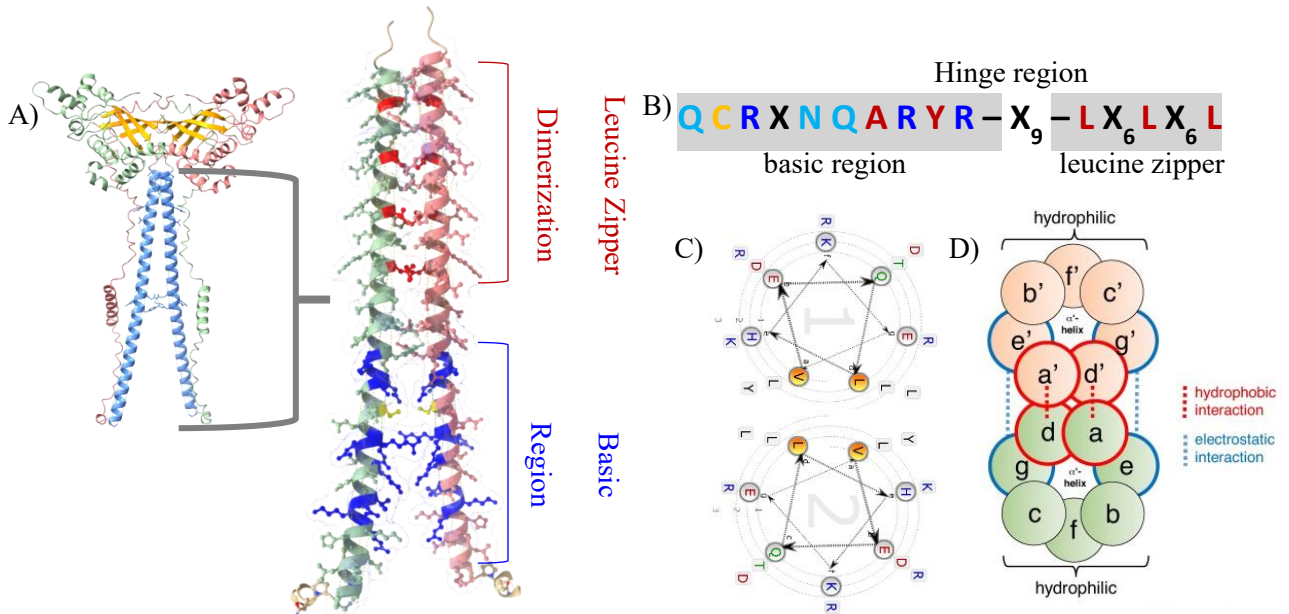


Figure 19: Analysis of *P. pluvialis* PPZIP14

The leucine zipper and DNA binding domain of the PPZIP14 was analysed in more detail. A) Overview of the PPZIP14 protein model on the left. On the right details of the ZIP domain are shown. The leucine zipper and basic region are shown. Leucine (red), Arginine (blue) and Cysteine (yellow) residues have been indicated in the structure. B) Sequence of the leucine zipper domain, hinge region and basic region. C) Helical wheel view of the leucine zipper domain of bZIP14 based on paircoil2 analysis (<https://waggawagga.motorprotein.de/>). On basis of the interacting residues a score is calculated (Single-Alpha-Helix Score), which enables to discriminate between predicted coiled-coil regions and a Single-Alpha-Helix (SAH). A high SAH-score (values ≥ 0.25) for the selected protein sequence region is a strong indicator for a single- α -helix instead of a predicted coiled-coil. The SAH-Score for bZIP14 of 0.0442 (AA 5-22) confirms a coiled-coil structure D) General leucine zipper organization in bZIP proteins.

Chapter 4. Discussion

4.1. Mycelium growth

So far, our understanding of abiotic stress effects on pathogens is limited. The experiments conducted focused on temperature, salinity, and drought stress effects because of their known and severe effects on plant hosts. Furthermore, all of these abiotic factors are known to be directly associated with changing climate, hence will greatly impact future agriculture, forestry, and native ecosystems. The main aim of this project was to gain insight on how temperature changes, water limitation and osmotic stress impact the mycelial growth of different *P. pluvialis* strains. Current protocols used to grow *P. pluvialis* on media suggests growing the oomycete on carrot or V8 agar at a temperature range of 15°C to 20°C, however, most commonly it is grown at a constant temperature of 17°C[8,16]

Analysis of mycelial growth over time suggests that *P. pluvialis* optimum temperature varies between the different strains. Temperature between 15°C and 21°C studied do not pose a vast impact on the growth rate. However, higher growth rates are observed during optimum temperatures for each strain, for example 4015 having a higher growth rate at 20°C as opposed to 18°C (Figure 5). Statistical data supports this by showing that *P. pluvialis* mycelial growth rate is impacted by strain rather than temperature. *Phytophthora* spp, including *P. infestans*, *Phytophthora kernoviae* and *Phytophthora ramorum*, have been observed having optimal mycelium growth temperatures that are strain specific.[97–99]. The present data also supports the current *P. pluvialis* growth protocol of cultivating unknown *P. pluvialis* strains at a range of 15°C-20°C [8,16], but suggests that for optimal growth rate a consistent optimum temperature needs to be applied to visualise efficient growth. Future experiments will include additional replicates, but also more extreme temperature at the higher spectrum, e.g. 25°C, 28 and 30°C., which will be of particular interest in respect to a changing climate.

Aside of temperature changes, osmotic stress has been regularly associated with drought stress, industrial impact, and anthropologically induced changes. Mycelium exposed to increase in salinity generally lead to the decline of mycelium growth[100,101] . This effect was supported by *P. pluvialis*'s decline in mycelial growth during high exposure to salinity stress. Statistical analysis determined that growth rates are dependent on strains and NaCl concentrations. This could potentially be used as a treatment to prevent RNC caused by *P. pluvialis*; however, previous studies have shown evidence of *Phytophthora parasitic* and *Phytophthora cryptogea* increasing the severity of root rot as salinity increases, in tomatoes, citrus and chrysanthemum, respectively [74,76,102]. Although, the mentioned *Phytophthora* spp. fall under clade 1 and 8 and are not in the same clade 3 as *P. pluvialis*, this data might suggest clade specific traits. For future studies clade specific traits could be analysed comparing all clade 3 *Phytophthora* spp. [22,23]. Nevertheless, the *P. pluvialis* tolerance shown within the experiments lets us hypothesise that *Phytophthora* species might have a higher tolerance for osmotic stress than their host plants. This would explain why treatment with salts have been observed to be of disadvantage for the host plant.

Surprisingly the conducted experiments have shown that mycelium growth rate was unaffected by the increase in PEG concentration. However, statistical data shows that growth rate is dependent on *P. pluvialis* strain and concentration of PEG. In regards to *Phytophthora* spp. resistant to osmotic stress via PEG and its effects on mycelium growth appears to be species specific. It has been identified that *Phytophthora cambivora*, *Phytophthora cinnamomic*, *Phytophthora citricola* and *Phytophthora quercina* exposed to PEG 6000 (average Mn: 6000) exhibit mycelium growth inhibition by osmotic potential as opposed to strains grown on PEG 3350 (average Mn: 3350) [77]. The decline in mycelium growth due to PEG induced drought stress is not limited to oomycetes, studies have observed this pattern in fungi, mycelium growth was significant inhibited following high concentration exposure to PEG 6000[103,104]. Inhibition of growth is not limited to filamentous pathogens, exposure to high levels of PEG 6000-7000 have indicated an inhibition in the plant root hair growth [105]. The data from this experiment concludes that *P. pluvialis* is relatively resilient to of drought stress induced by PEG 3350.

However, due to the statistical and observational data inconsistencies, to be able to conclude that *P. pluvialis* is in fact tolerant of drought stress, further testing would need to be conducted with higher concentrations and higher PEG molecular weight (PEG 6000).

4.2. Expression of PpR01 and bZIP, PPZIP 07 under abiotic stress

RT-qPCR can be a powerful tool for the identification of gene expression due to its high sensitivity, speed, consistency, and specificity [106]. The key goal of this section of the research was to understand the relationship between abiotic stress, pathogenicity, and growth. To identify genes associated with pathogenicity and growth, RT-qPCR was performed on NaCl, and PEG treated *P. pluvialis* mycelium. The expression quantification of the RxLR effector, PpR01 involved in pathogenicity, bZIP transcription factors, PPZIP 07 involved in mycelium growth and the reference gene actin were assessed.

Analysis of expression levels of PpR01 and PPZIP 07 during NaCl induced salinity stress on *P. pluvialis* mycelium found that PpR01 and PPZIP 07 are marginally expressed. These findings conclude that pathogenicity and growth is hindered by exposure to salinity stress. The inhibited growth rate is supported by the findings in Section 3.2.1., which shows a growth rate decline during exposure to high levels of NaCl. However, this data conflicts with studies showing an increase infection of *Phytophthora* spp. as salinity increases [74]. The current data was normalized using actin as a reference gene and shows that high salinity does affect the expression of PPZIP 07 involved in mycelium growth, therefore inhibiting growth, in turn, affecting the expression of RxLR effector, PpR01 and eliminating pathogenicity of *P. pluvialis* onto host plant.

Alternatively, expression of PpR01 and PPZIP 07 during PEG induced drought stress revealed an upregulation for both genes. The expression results indicate that pathogenicity and growth are not

inhibited by PEG exposure. Section 3.2.2 supports the findings, showing that growth is not influenced by the concentration of PEG applied to *P. pluvialis* mycelium. In *Phytophthora* spp. pathogenicity and growth are increased during an increase in drought stress applied to the host plant [77]. These findings were normalized using actin as a reference gene and suggest that *P. pluvialis* pathogenicity and growth are unaffected by the presence of PEG, which could indicate resistance to drought stress.

Current research examining the expression of oomycete pathogenicity gene in relation to abiotic stress, are performed on the infected host plant undergoing abiotic stress [78]. This provides a more accurate representation of effector expression in nature. Further studies should utilize the current findings of this thesis and applying abiotic stresses to *P. pluvialis* infected *P. radiata* to accurately determine reproducibility of the data. In addition, the inclusion of other reference gene(s) will prevent the occurrence of single reference gene normalization error. COX1 and COX2 (already tested) are highly conserved genes identified in *Phytophthora* spp and are commonly used as internal standards or reference genes [107,108]. In this experiment, COX2 was attempted to be used as a reference gene, but the primers developed were unsuccessful (Figure 11b).

4.3. Phylogenetic analysis of *P. pluvialis* bZIPs

This section of the research focused on the use of computational phylogenetic analysis to identify conserved *P. pluvialis* bZIPs. The aim was to identify novel *P. pluvialis* bZIPs from highly conserved *P. infestans* bZIPs, theorise their function and identify using previously identified bZIP TFs of *P. infestans* from Gamboa-Melendez et al, and *Phytophthora* spp. phylogenetic analysis by Yang et al, as a foundation [23,91].

Computational analysis using novel *P. pluvialis* bZIPs to develop a RAxML phylogenetic trees revealed that *P. pluvialis* is more closely related to *Phytophthora pseudosyringae* in contrast to *P. infestans*. This

data reinforces the currently established *Phytophthora* spp. phylogenetic tree, as *P. pluvialis* fall under clade 3, along with *Phytophthora psychrophilia*, *Phytophthora ilicis*, *Phytophthora nemorosa* and *Phytophthora pseudosyringae* [23]. Studies have suggested that members of clade 3, *P. nemorosa* and *P. pseudosyringae* have similar host ranges[109]. The current findings from this research could be used toward future infection studies to determine if *P. pluvialis* and *P. pseudosyringae*, may infect the same or similar hosts or have a similar infection pattern. With the recent discovery of *P. pluvialis* acquiring a new host and infecting the Western Hemlock in the UK [28], competition studies could be performed to determine if competition occurs between the clades.

bZIPs for *P. pluvialis* are currently unknown, using current data of *P. infestans* bZIPs and phylogenetic analysis revealed 29 *P. pluvialis* bZIPs that are theorised to be expressed during mycelial growth, production of sporangia, zoospore germination and infection [91]. This is following the assumption that the function of these novel bZIPs is similar to that of already know *P. infestans* bZIPs. Future testing would be required to determine their definite function. While performing phylogenetic analysis of bZIP sequence alignments for *P. pluvialis* and *P. infestans*, multiple bZIP TF sequences of *P. infestans* appeared to be present in the same genome sequence as *P. pluvialis* (Table 11). This shows that *P. pluvialis* may contain fewer number of genome sequences required to perform similar functions to *P. infestans*. Alternatively, one genome sequence may have multiple functions on the same sequence as opposed to *P. infestans*.

In addition to the phylogenetic analysis, protein models allowed some novel insight into the potential structures of a group of *P. pluvialis* bZIP transcription factors. Aside of the conserved Leucin zipper domain, followed by the basic DNA interaction domain protein models indicated a high complexity of bZIP proteins. The analysed group of bZIPs contained a conserved beta sheet and multiple alpha helices coordinating the head group of the transcription factor. Interestingly, the function of such a head group is not known yet but has been predicted for plant ZIPs as well. Hence it will be of interest to further

analyse how far these structures are conserved within oomycetes, and within eukaryotes and their molecular and biological function.

Chapter 5. Conclusion

5.1. Future directions

In addition to the future of this research mentioned previously, an expansion to this current thesis could be accomplished by exposing abiotic stress onto *P. radiata* trees during *P. pluvialis* infection and monitoring adaptations and change in gene expression. In addition to understanding host and pathogen adaptations, research could be conducted to easily identify and detect *P. pluvialis* in other parts of New Zealand and the world.

With the recent identification of *P. pluvialis* in the United Kingdom, *P. pluvialis* is predicted to become more recognized worldwide. Which will allow and increase interest for further studies into its identification, genome, adaptations, and mutations. The introduction of a new host, Western Hemlock, raises global concern if *P. pluvialis* has a wider host range than previously known, or was there an event that may have reduced native pathogen competition for *P. pluvialis*.

In regard to climate change, further study can be done to understand possible environmental adaptations that may have occurred due to selection pressure or natural disaster. Moreover, further research involving other abiotic stresses, including humidity, heat or ultraviolet (UV) could be performed.

5.2. Concluding remarks

Phytophthora species are filamentous pathogens that have caused disruption to food security and natural resources globally for centuries. With the current predictions of climate change, global environments are predicted shift drastically which may lead to mutations and adaptation in plant pathogens as a result

of environmental selection pressure. This could result in pathogens migration to different environments, infecting novel hosts and resistance development.

This thesis investigated three environmental factors (drought and osmotic stress) that commonly occur in nature and their effects on the pathogen *P. pluvialis*. Here we show observational, statistical and gene expression evidence of *P. pluvialis* mycelial growth being negatively affected during salinity stress, while mycelial growth was unaffected during PEG induced drought stress. In addition, gene expression data analysis of RxLR effector, PpR01, revealed that pathogenicity may be increased by drought stress, while it is inhibited during salinity stress.

To further understand the relationship between *P. pluvialis* and *Phytophthora* spp., novel *P. pluvialis* bZIPs were identified. Phylogenetic analysis of bZIP transcription factors confirmed *P. pseudosyringae* being a sister group, sharing the same common ancestor as *P. pluvialis*.

The information in this research will hopefully provide more insight into *P. pluvialis* and its reaction and adaptation to abiotic stress. Including the position and theorized function of *P. pluvialis* bZIPs for future research.

Bibliography

- 1 Sogin, M.L. and Silberman, J.D. (1998) Evolution of the protists and protistan parasites from the perspective of molecular systematics. *International Journal for Parasitology* 28, 11–20
- 2 Agrios, G.N. (1988) Introduction to plant pathology. *Plant pathology*
- 3 Tucker, C.M. and Milbrath, J.A. (1942) Root Rot of *Chamaecyparis* Caused by a Species of *Phytophthora*. *Mycologia* 34, 94
- 4 Kroon, L.P.N.M. *et al.* (2012) The Genus *Phytophthora* Anno 2012. *Phytopathology*® 102, 348–364
- 5 Goheen, E.M. and Frankel, S.J. (2009) *Proceedings of the fourth meeting of the International Union of Forest Research Organizations (IUFRO) Working Party S07.02.09: Phytophthoras in forests and natural ecosystems*, U.S. Department of Agriculture, Forest Service, Pacific Southwest Research Station.
- 6 Batuman, O. *et al.* (2020) Chapter 17 - Diseases caused by fungi and oomycetes. In *The Genus Citrus* (Talon, M. *et al.*, eds), pp. 349–369, Woodhead Publishing
- 7 Schumann, G.L. (1991) *Plant diseases: their biology and social impact.*, APS press.
- 8 Dick, M.A. *et al.* (2014) Pathogenicity of *Phytophthora pluvialis* to *Pinus radiata* and its relation with red needle cast disease in New Zealand. *New Zealand Journal of Forestry Science* 44, 6
- 9 Hansen, E.M. (2015) *Phytophthora* Species Emerging as Pathogens of Forest Trees. *Curr Forestry Rep* 1, 16–24
- 10 Kamoun, S. (2009) Plant Pathogens: Oomycetes (water mold). In *Encyclopedia of Microbiology* pp. 689–695, Elsevier
- 11 Eccersall, S.E. (2021) Identifying *Phytophthora pluvialis* effector targets in *Pinus radiata*. DOI: 10.26021/11077
- 12 Hardina, N. *et al.* (2020) Modified vegetables extract as substitution of v8-juice medium for cultivation of *Phytophthora* spp. *IOP Conference Series: Earth and Environmental Science* 486, 012149
- 13 Brar, S. *et al.* (2018) Genetic diversity of *Phytophthora pluvialis*, a pathogen of conifers, in New Zealand and the west coast of the United States of America. *Plant Pathology* 67, 1131–1139
- 14 Tabima, J.F. *et al.* (2021) Molecular Phylogenomics and Population Structure of *Phytophthora pluvialis*. *Phytopathology*® 111, 108–115

- 15 Welsh Government 13-Dec-(2021) , First case of tree disease *Phytophthora pluvialis* discovered in Wales.
- 16 Reeser, P. (2013) *Phytophthora pluvialis*, a new species from mixed tanoak-Douglas-fir forests of western Oregon, U.S.A. *North Amer. Fun.* DOI: 10.2509/naf2013.008.007
- 17 Reeser, P. *et al.* (2015) *Phytophthora pluvialis*. *For Phytophthoras* 5,
- 18 H Ho, H. (2018) The Taxonomy and Biology of *Phytophthora* and *Pythium*. *JBMOA* 6,
- 19 Zuluaga, A.P. *et al.* (2015) Transcriptional dynamics of *Phytophthora infestans* during sequential stages of hemibiotrophic infection of tomato. *Mol Plant Pathol* 17, 29–41
- 20 Le Fevre, R. *et al.* (2016) Colonization of Barley by the Broad-Host Hemibiotrophic Pathogen *Phytophthora palmivora* Uncovers a Leaf Development–Dependent Involvement of Mlo. *MPMI* 29, 385–395
- 21 Cooke, D. *et al.* (2000) A molecular phylogeny of *Phytophthora* and related oomycetes. *Fungal genetics and biology* 30, 17–32
- 22 Blair, J.E. *et al.* (2008) A multi-locus phylogeny for *Phytophthora* utilizing markers derived from complete genome sequences. *Fungal Genetics and Biology* 45, 266–277
- 23 Yang, X. *et al.* (2017) An expanded phylogeny for the genus *Phytophthora*. *IMA Fungus* 8,
- 24 Hansen, E.M. *et al.* (2015) First Report of *Phytophthora pluvialis* Causing Needle Loss and Shoot Dieback on Douglas-fir in Oregon and New Zealand. *Plant Disease* 99, 727–727
- 25 Berg, Peter (2008) Radiata pine - Plantations in New Zealand. *Te Ara - the Encyclopedia of New Zealand*
- 26 McDougal, R.L. *et al.* (2021) Molecular detection of *Phytophthora pluvialis*, the causal agent of red needle cast in *Pinus radiata*. *Journal of Microbiological Methods* 189, 106299
- 27 Forest Research (2021) *Phytophthora pluvialis* symptom guide (western hemlock). at https://assets.publishing.service.gov.uk/government/uploads/system/uploads/attachment_data/file/1029958/Symptom_guide_P_pluvialis_final_21-10-29.pdf
- 28 First report of *Phytophthora pluvialis* in Europe causing resinous cankers on western hemlock - Pérez-Sierra - 2022 - New Disease Reports - Wiley Online Library. . [Online]. Available: <https://bsppjournals.onlinelibrary.wiley.com/doi/full/10.1002/ndr2.12064>. [Accessed: 26-Feb-2022]
- 29 Ministry for Primary Industries (2019) National Exotic Forest Description.
- 30 Ministry for Primary Industries (2021) Human capability in the primary industries data: Part 1.

- 31 Brasov, P. and Killerby, S. (2011) Promotion of wood and forest products in New Zealand.
- 32 Forestry New Zealand Wood product markets. . (2018)
- 33 Ganley, R.J. *et al.* (2014) Management of red needle cast caused by *Phytophthora pluvialis* a new disease of radiata pine in New Zealand. *NZPP* 67, 48–53
- 34 Kanaskie, A. *et al.* (2011) Application of phosphonate to prevent sudden oak death in south-western Oregon tanoak (*Notholithocarpus densiflorus*) forests. *New Zealand Journal of Forestry Science*
- 35 Shearer, B.L. and Crane, C.E. (2009) Influence of site and rate of low-volume aerial phosphite spray on lesion development of *Phytophthora cinnamomi* and phosphite persistence in *Lambertia inermis* var. *inermis* and *Banksia grandis*. *Austral. Plant Pathol.* 38, 288
- 36 Mohammadi, M.A. *et al.* (2021) ROS and Oxidative Response Systems in Plants Under Biotic and Abiotic Stresses: Revisiting the Crucial Role of Phosphite Triggered Plants Defense Response. *Frontiers in Microbiology* 12,
- 37 Filho, J.A.C. *et al.* (2016) Mycorrhizal Association and Their Role in Plant Disease Protection. In *Plant, Soil and Microbes* (Hakeem, K. R. and Akhtar, M. S., eds), pp. 95–143, Springer International Publishing
- 38 Hoitink, H.A.J. *et al.* (2006) Systemic Resistance Induced by *Trichoderma* spp.: Interactions Between the Host, the Pathogen, the Biocontrol Agent, and Soil Organic Matter Quality. *Phytopathology*® 96, 186–189
- 39 Ozyilmaz, U. and Benlioglu, K. (2013) Enhanced biological control of phytophthora blight of pepper by biosurfactant-producing pseudomonas. *Plant Pathol J* 29, 418–426
- 40 Plant Disease - an overview | ScienceDirect Topics. . [Online]. Available: <https://www.sciencedirect.com/topics/medicine-and-dentistry/plant-disease>. [Accessed: 09-Mar-2022]
- 41 Morris, W.F. *et al.* (2020) Biotic and anthropogenic forces rival climatic/abiotic factors in determining global plant population growth and fitness. *Proceedings of the National Academy of Sciences* 117, 1107–1112
- 42 Teshome, D.T. *et al.* (2020) The Threat of the Combined Effect of Biotic and Abiotic Stress Factors in Forestry Under a Changing Climate. *Frontiers in Plant Science* 11,
- 43 Snowdon, R.J. *et al.* (2021) Crop adaptation to climate change as a consequence of long-term breeding. *Theor Appl Genet* 134, 1613–1623

- 44 Ruehr, N.K. *et al.* (2019) Beyond the extreme: recovery of carbon and water relations in woody plants following heat and drought stress. *Tree Physiology* 39, 1285–1299
- 45 Froux, F. *et al.* (2005) Vulnerability to embolism differs in roots and shoots and among three Mediterranean conifers: consequences for stomatal regulation of water loss? *Trees* 19, 137–144
- 46 Sperry, J.S. (1986) Relationship of Xylem Embolism to Xylem Pressure Potential, Stomatal Closure, and Shoot Morphology in the Palm *Rhapis excelsa* 1. *Plant Physiology* 80, 110–116
- 47 Nguyen, A. and Lamant, A. (1989) Variation in growth and osmotic regulation of roots of water-stressed maritime pine (*Pinus pinaster* Ait.) provenances. *Tree Physiology* 5, 123–133
- 48 Munné-Bosch, S. and Alegre, L. (2004) Die and let live: leaf senescence contributes to plant survival under drought stress. *Functional Plant Biol.* 31, 203–216
- 49 Munns, R. and Termaat, A. (1986) Whole-plant responses to salinity. *Functional Plant Biology* 13, 143–160
- 50 Zhu, J.K. (2001) Plant salt tolerance. *Trends Plant Sci* 6, 66–71
- 51 Tester, M. and Davenport, R. (2003) Na⁺ tolerance and Na⁺ transport in higher plants. *Ann Bot* 91, 503–527
- 52 Tsugane, K. *et al.* (1999) A recessive Arabidopsis mutant that grows photoautotrophically under salt stress shows enhanced active oxygen detoxification. *The Plant Cell* 11, 1195–1206
- 53 Munns, R. and Tester, M. (2008) Mechanisms of salinity tolerance. *Annu. Rev. Plant Biol.* 59, 651–681
- 54 Harfouche, A. *et al.* (2014) Molecular and physiological responses to abiotic stress in forest trees and their relevance to tree improvement. *Tree Physiology* 34, 1181–1198
- 55 Zhu, J.-K. (2003) Regulation of ion homeostasis under salt stress. *Current opinion in plant biology* 6, 441–445
- 56 Asada, K. (1999) THE WATER-WATER CYCLE IN CHLOROPLASTS: Scavenging of Active Oxygens and Dissipation of Excess Photons. *Annual Review of Plant Physiology and Plant Molecular Biology* 50, 601–639
- 57 Tisi, A. *et al.* (2008) Wound healing in plants: cooperation of copper amine oxidase and flavin-containing polyamine oxidase. *Plant signaling & behavior* 3, 204–206

- 58 Navakoudis, E. *et al.* (2003) Ozone impact on the photosynthetic apparatus and the protective role of polyamines. *Biochimica et Biophysica Acta (BBA)-General Subjects* 1621, 160–169
- 59 Salehi-Lisar, S.Y. and Bakhshayeshan-Agdam, H. (2016) Drought Stress in Plants: Causes, Consequences, and Tolerance. In *Drought Stress Tolerance in Plants, Vol 1* (Hossain, M. A. *et al.*, eds), pp. 1–16, Springer International Publishing
- 60 Yamaguchi-Shinozaki, K. and Shinozaki, K. (2006) Transcriptional regulatory networks in cellular responses and tolerance to dehydration and cold stresses. *Annu Rev Plant Biol* 57, 781–803
- 61 Gollmack, D. *et al.* (2014) Tolerance to drought and salt stress in plants: Unraveling the signaling networks. *Front Plant Sci* 5, 151
- 62 Newman, M.-A. *et al.* (2013) MAMP (microbe-associated molecular pattern) triggered immunity in plants. *Frontiers in plant science* 4, 139
- 63 Zipfel, C. and Robatzek, S. (2010) Pathogen-associated molecular pattern-triggered immunity: *veni, vidi...?* *Plant physiology* 154, 551–554
- 64 Ali, M. and Baek, K.-H. (2020) Jasmonic acid signaling pathway in response to abiotic stresses in plants. *International Journal of Molecular Sciences* 21, 621
- 65 Horváth, E. *et al.* (2007) Induction of Abiotic Stress Tolerance by Salicylic Acid Signaling. *J. Plant Growth Regul.* 26, 290–300
- 66 Kazan, K. (2015) Diverse roles of jasmonates and ethylene in abiotic stress tolerance. *Trends Plant Sci* 20, 219–229
- 67 Sah, S.K. *et al.* (2016) Abscisic Acid and Abiotic Stress Tolerance in Crop Plants. *Frontiers in Plant Science* 7,
- 68 Judelson, H.S. and Ah-Fong, A.M.V. (2019) Exchanges at the Plant-Oomycete Interface That Influence Disease1[OPEN]. *Plant Physiol* 179, 1198–1211
- 69 Whisson, S.C. *et al.* (2007) A translocation signal for delivery of oomycete effector proteins into host plant cells. *Nature* 450, 115–118
- 70 Bostock, R.M. *et al.* (2014) Predisposition in plant disease: exploiting the nexus in abiotic and biotic stress perception and response. *Annual review of phytopathology* 52, 517–549

- 71 Huot, B. *et al.* (2017) Dual impact of elevated temperature on plant defence and bacterial virulence in *Arabidopsis*. *Nat Commun* 8, 1808
- 72 Robinson, C.H. (2001) Cold adaptation in Arctic and Antarctic fungi. *New Phytologist* 151, 341–353
- 73 Deliopoulos, T. *et al.* (2010) Fungal disease suppression by inorganic salts: a review. *Crop Protection* 29, 1059–1075
- 74 MacDonald, J. *et al.* (1984) Effects of salinity stress on the development of *Phytophthora* root rots. *California Agriculture* 38, 23–24
- 75 Liu, Y. *et al.* (2021) Effect of Osmotic Stress on the Growth, Development and Pathogenicity of *Setosphaeria turcica*. *Frontiers in Microbiology* 12,
- 76 Blaker, N. and MacDonald, J. (1986) The role of salinity in the development of *Phytophthora* root rot of citrus. *Phytopathology* 76, 970–975
- 77 Turco, E. *et al.* (2005) Effect of polyethylene glycol and composition of basal medium on the mycelial growth of *Phytophthora* spp./Wirkung von Polyethylenglycol und der Zusammensetzung des Basalmediums auf das Mycelwachstum von *Phytophthora* spp. *Zeitschrift für Pflanzenkrankheiten und Pflanzenschutz/Journal of Plant Diseases and Protection*
- 78 Gupta, A. *et al.* (2016) Drought Stress Predominantly Endures *Arabidopsis thaliana* to *Pseudomonas syringae* Infection. *Frontiers in Plant Science* 7,
- 79 Getting specific | Nature Reviews Molecular Cell Biology. . [Online]. Available: <https://www.nature.com/articles/milegene11>. [Accessed: 06-Mar-2022]
- 80 Yin, Y. *et al.* (1997) RF2a, a bZIP transcriptional activator of the phloem-specific rice tungro bacilliform virus promoter, functions in vascular development. *The EMBO Journal* 16, 5247–5259
- 81 Weltmeier, F. *et al.* (2006) Combinatorial control of *Arabidopsis* proline dehydrogenase transcription by specific heterodimerisation of bZIP transcription factors. *The EMBO Journal* 25, 3133–3143
- 82 Ulm, R. *et al.* (2004) Genome-wide analysis of gene expression reveals function of the bZIP transcription factor HY5 in the UV-B response of *Arabidopsis*. *Proceedings of the National Academy of Sciences* 101, 1397–1402

- 83 Satoh, R. *et al.* (2004) A novel subgroup of bZIP proteins functions as transcriptional activators in hypoosmolarity-responsive expression of the ProDH gene in Arabidopsis. *Plant and Cell Physiology* 45, 309–317
- 84 Karin, M. (1990) Too many transcription factors: positive and negative interactions. *The New Biologist* 2, 126–131
- 85 Hurst, H.C. (1994) Transcription factors. 1: bZIP proteins. *Protein Profile* 1, 123–168
- 86 Landschulz, W.H. *et al.* (1988) The Leucine Zipper: A Hypothetical Structure Common to a New Class of DNA Binding Proteins. *Science* 240, 1759–1764
- 87 Vinson, C.R. *et al.* (1989) Scissors-Grip Model for DNA Recognition by a Family of Leucine Zipper Proteins. *Science* 246, 911–916
- 88 Fry, W. (2008) Phytophthora infestans: the plant (and R gene) destroyer. *Mol Plant Pathol* 9, 385–402
- 89 Hildebrand, A.A. (1959) A ROOT AND STALK ROT OF SOYBEANS CAUSED BY PHYTOPHTHORA MEGASPERMA DRECHSLER VAR. SOJAE VAR. NOV. *Can. J. Bot.* 37, 927–957
- 90 Kaufmann, M.J. (1957) *Root and stem rot of soybean caused by Phytophthora sojae n. sp.*, University of Illinois at Urbana-Champaign.
- 91 Gamboa-Meléndez, H. *et al.* (2013) bZIP Transcription Factors in the Oomycete Phytophthora infestans with Novel DNA-Binding Domains Are Involved in Defense against Oxidative Stress. *Eukaryot Cell* 12, 1403–1412
- 92 Möglich, A. *et al.* (2009) Structure and signaling mechanism of Per-ARNT-Sim domains. *Structure* 17, 1282–1294
- 93 Sheng, Y. *et al.* (2021) The bZIP transcription factor PsBZP32 is involved in cyst germination, oxidative stress response, and pathogenicity of Phytophthora sojae. *Phytopathology Research* 3, 1
- 94 P.infestans actin (actA) gene, complete cds. . 18-Jul-(1991)
- 95 P.infestans actin (actB) gene, complete cds. . 18-Jul-(1991)
- 96 Mirdita, M. *et al.* ColabFold - Making protein folding accessible to all. . 08-Feb-(2022) , bioRxiv, 2021.08.15.456425

- 97 Maziero, J.M.N. *et al.* (2009) Effects of temperature on events in the infection cycle of two clonal lineages of *Phytophthora infestans* causing late blight on tomato and potato in Brazil. *Plant Disease* 93, 459–466
- 98 Shelley, B.A. *et al.* (2018) Effects of temperature on germination of sporangia, infection and protein secretion by *Phytophthora kernoviae*. *Plant Pathology* 67, 719–728
- 99 Browning, M. *et al.* (2008) Survival of *Phytophthora ramorum* Hyphae after Exposure to Temperature Extremes and Various Humidities. *Mycologia* 100, 236–245
- 100 Venâncio, C. *et al.* (2017) Salinity induced effects on the growth rates and mycelia composition of basidiomycete and zygomycete fungi. *Environmental Pollution* 231, 1633–1641
- 101 Effects of Two Salts Compounds on Mycelial Growth, Sporulation, and Spore Germination of Six Isolates of *Botrytis cinerea* in the Western North of Algeria. . [Online]. Available: <https://www.hindawi.com/journals/ijmicro/2015/572626/>. [Accessed: 20-Mar-2022]
- 102 Swiecki, T.J. and MacDonald, J.D. (1991) Soil Salinity Enhances *Phytophthora* Root Rot of Tomato but Hinders Asexual Reproduction by *Phytophthora parasitica*. *Jashs* 116, 471–477
- 103 Liu, B. *et al.* (2021) Stress tolerance of *Xerocomus badius* and its promotion effect on seed germination and seedling growth of annual ryegrass under salt and drought stresses. *AMB Express* 11, 15
- 104 Zhang, H.-H. *et al.* (2011) The response of ectomycorrhizal (ECM) fungi under water stress induced by polyethylene glycol (PEG) 6000. *African Journal of Microbiology Research* 5, 365–373
- 105 Zahran, H.H. and Sprent, J.I. (1986) Effects of sodium chloride and polyethylene glycol on root-hair infection and nodulation of *Vicia faba* L. plants by *Rhizobium leguminosarum*. *Planta* 167, 303–309
- 106 Gachon, C. *et al.* (2004) Real-time PCR: what relevance to plant studies? *Journal of Experimental Botany* 55, 1445–1454
- 107 Martin, F.N. *et al.* (2004) Molecular Detection of *Phytophthora ramorum*, the Causal Agent of Sudden Oak Death in California, and Two Additional Species Commonly Recovered from Diseased Plant Material. *Phytopathology* 94, 621–631
- 108 Martin, F. *et al.* (2009) Evaluation of Molecular Markers for *Phytophthora ramorum* Detection and Identification: Testing for Specificity Using a Standardized Library of Isolates. *Phytopathology* 99, 390–403

109 Australian Department of Agriculture and Water Resources (2015) Final review of policy: importation of *Phytophthora ramorum* host propagative material into Australia. CC BY 3.0.

Supplemental

V8 tomato ingredients:

- Tomatoes
- Carrots
- Beetroot
- Celery
- Lettuce
- Parsley
- Spinach
- Watercress

10% V8 broth:

For 1000 mL

Milli-Q	900 mL
V8 juice	100 mL
Calcium carbonate (CaCO ₃)	3g

Supplementary Table 1: 10% V8 broth recipe

10% V8 agar:

For 1000 mL

Milli-Q	900 mL
V8 juice	100 mL
Calcium carbonate (CaCO ₃)	3g
Biological grade agar-agar powder	15g

Supplementary Table 2: 10% V8 agar recipe.

Altered 10% V8 media with the addition of NaCl and PEG

For 1000 mL

NaCl and PEG concentration/ [% w/v]	Amount of NaCl and PEG/ [g]
1	10
2	20
3	30
4	40
5	50

Supplementary Table 3: Alter 10% V8 media

Primer	Forward sequence (5'-3')	Reverse sequence (5'-3')
PPR01-1	AAGCATTCCCCGTATCACG	TCTTCGTCGTCTTGGCATC
PPR01-2	ATCGATAAGCTCCTTGCCGC	CAACTTTCATTCCGGTCGCG
PPR01-3	GGCCGAGAAGTTGAACATGC	CCAGAAGAGGAAGTCTGCGT
PPR01-4	GCCGAGAAGTTGAACATGCC	AGAAGAGGAAGTCTGCGTCG
PACT-1	CGACCTGCGCCTTAGTGAAA	GCCCATTTTCGTCGGTTTGAG
PACT-2	ATGGGTCGGGTATGTGCAAG	AAGCACTTGGGCATCATGGT
BZIP-1	ATCTCAGCGTGGATGGAAGC	TGTTTTCCAGCGTCCTCCTC
BZIP-2	CCAGGAAACGTCAAGACCGA	CCCAGAAGAGTGACGCAGTG
BZIP-3	ATCAAATCACGGGCCAGCT	GCGATCACATGCCCCATTG
BZIP-4	CAGAGTCCGTGGTCTAT	AGGAGATGAAAAGCCAC
COX 2	TTCCGGCAACCATTGTACATG	GCAAAAAGAGGGTACAGCAAC

Supplementary Table 4: Forward and reverse primers for PpR01, BZIP and COX2

Mycelium grown at varying temperatures.

```
> res.aov4<-aov(growth~strain+temp+strain:temp,data=rstudio)
> summary(res.aov4)
      Df Sum Sq Mean Sq F value Pr(>F)
strain  4 1629.4   407.3  176.638 <2e-16 ***
temp    6   21.8     3.6    1.574  0.162
strain:temp 24   65.5     2.7    1.184  0.274
Residuals 105  242.1     2.3
---
Signif. codes:  0 '***' 0.001 '**' 0.01 '*' 0.05 '.' 0.1 ' ' 1
```

Supplementary Figure 1

```
> TukeyHSD(res.aov4, which="strain")
Tukey multiple comparisons of means
95% family-wise confidence level

Fit: aov(formula = growth ~ strain + temp + strain:temp, data = rstudio)

$strain
      diff      lwr      upr      p adj
3618-3000 4.2578817  3.1313254  5.384438 0.0000000
3632-3000 6.2096942  5.0831379  7.336250 0.0000000
3880-3000 0.8642522 -0.2623040  1.990808 0.2155041
4015-3000 9.2416496  8.1150933 10.368206 0.0000000
3632-3618 1.9518125  0.8252562  3.078369 0.0000494
3880-3618 -3.3936295 -4.5201857 -2.267073 0.0000000
4015-3618 4.9837679  3.8572116  6.110324 0.0000000
3880-3632 -5.3454420 -6.4719982 -4.218886 0.0000000
4015-3632 3.0319554  1.9053991  4.158512 0.0000000
4015-3880 8.3773973  7.2508411  9.503954 0.0000000
```

Supplementary Figure 2

```
> TukeyHSD(res.aov4, which="temp")
Tukey multiple comparisons of means
95% family-wise confidence level

Fit: aov(formula = growth ~ strain + temp + strain:temp, data = rstudio)

$temp
      diff      lwr      upr      p adj
16-15 -0.27820000 -1.72186365  1.1654637 0.9972748
17-15 -0.67625938 -2.11992303  0.7674043 0.7962659
18-15 -0.23674375 -1.68040740  1.2069199 0.9988995
19-15  0.02596875 -1.41769490  1.4696324 1.0000000
20-15 -0.26706875 -1.71073240  1.1765949 0.9978296
21-15  0.70805625 -0.73560740  2.1517199 0.7592075
17-16 -0.39805937 -1.84172303  1.0456043 0.9813964
18-16  0.04145625 -1.40220740  1.4851199 1.0000000
19-16  0.30416875 -1.13949490  1.7478324 0.9955416
20-16  0.01113125 -1.43253240  1.4547949 1.0000000
21-16  0.98625625 -0.45740740  2.4299199 0.3878518
18-17  0.43951562 -1.00414803  1.8831793 0.9693732
19-17  0.70222812 -0.74143553  2.1458918 0.7661969
20-17  0.40919062 -1.03447303  1.8528543 0.9785892
21-17  1.38431563 -0.05934803  2.8279793 0.0691649
19-18  0.26271250 -1.18095115  1.7063762 0.9980204
20-18 -0.03032500 -1.47398865  1.4133387 1.0000000
21-18  0.94480000 -0.49886365  2.3884637 0.4414365
20-19 -0.29303750 -1.73670115  1.1506262 0.9963670
21-19  0.68208750 -0.76157615  2.1257512 0.7896769
21-20  0.97512500 -0.46853865  2.4187887 0.4019650
```

Supplementary Figure 3

Mycelium growth under salinity stress

```
> summary(res.aov3)
      Df Sum Sq Mean Sq F value    Pr(>F)
strain  4  20.36    5.09  18.443 3.59e-07 ***
conc    4 191.42   47.85 173.437 < 2e-16 ***
strain:conc 16  40.62    2.54   9.201 7.64e-07 ***
Residuals 25   6.90    0.28
---
Signif. codes:  0 '***' 0.001 '**' 0.01 '*' 0.05 '.' 0.1 ' ' 1
```

Supplementary Figure 4

```
> TukeyHSD(res.aov3, which="conc")
  Tukey multiple comparisons of means
  95% family-wise confidence level

Fit: aov(formula = growth ~ strain + conc + strain:conc, data = rstudio)

$conc
      diff      lwr      upr    p adj
2-1 -1.81742 -2.5073291 -1.1275109 0.0000004
3-1 -4.10110 -4.7910091 -3.4111909 0.0000000
4-1 -4.89188 -5.5817891 -4.2019709 0.0000000
5-1 -5.02250 -5.7124091 -4.3325909 0.0000000
3-2 -2.28368 -2.9735891 -1.5937709 0.0000000
4-2 -3.07446 -3.7643691 -2.3845509 0.0000000
5-2 -3.20508 -3.8949891 -2.5151709 0.0000000
4-3 -0.79078 -1.4806891 -0.1008709 0.0190008
5-3 -0.92140 -1.6113091 -0.2314909 0.0049971
5-4 -0.13062 -0.8205291  0.5592891 0.9801505
```

Supplementary Figure 5

```
> TukeyHSD(res.aov3, which="strain")
  Tukey multiple comparisons of means
  95% family-wise confidence level

Fit: aov(formula = growth ~ strain + conc + strain:conc, data = rstudio)

$strain
      diff      lwr      upr    p adj
3618-3000 -0.28762 -0.977529114  0.4022891 0.7375913
3632-3000  0.88634  0.196430886  1.5762491 0.0072007
3880-3000  0.39484 -0.295069114  1.0847491 0.4631240
4015-3000  1.50244  0.812530886  2.1923491 0.0000100
3632-3618  1.17396  0.484050886  1.8638691 0.0003341
3880-3618  0.68246 -0.007449114  1.3723691 0.0535435
4015-3618  1.79006  1.100150886  2.4799691 0.0000005
3880-3632 -0.49150 -1.181409114  0.1984091 0.2545632
4015-3632  0.61610 -0.073809114  1.3060091 0.0963865
4015-3880  1.10760  0.417690886  1.7975091 0.0006846
```

Supplementary Figure 6

Mycelium growth under drought stress

```
> summary(res.aov3)
      Df Sum Sq Mean Sq F value    Pr(>F)
strain  4 1261.3   315.33  542.241 < 2e-16 ***
conc    4    7.3    1.83    3.152  0.0315 *
strain:conc 16  70.0    4.37    7.523 5.19e-06 ***
Residuals 25  14.5    0.58
---
Signif. codes:  0 '***' 0.001 '**' 0.01 '*' 0.05 '.' 0.1 ' ' 1
```

Supplementary Figure 7

```

> TukeyHSD(res.aov3, which="conc")
  Tukey multiple comparisons of means
    95% family-wise confidence level

Fit: aov(formula = growth ~ strain + conc + strain:conc, data = rstudio)

$conc
      diff          lwr          upr      p adj
2-1  0.40144 -0.60014602  1.403026  0.7640046
3-1  0.96762 -0.03396602  1.969206  0.0618981
4-1  0.79500 -0.20658602  1.796586  0.1684353
5-1  1.00796  0.00637398  2.009546  0.0480120
3-2  0.56618 -0.43540602  1.567766  0.4752188
4-2  0.39356 -0.60802602  1.395146  0.7765615
5-2  0.60652 -0.39506602  1.608106  0.4075689
4-3 -0.17262 -1.17420602  0.828966  0.9859879
5-3  0.04034 -0.96124602  1.041926  0.9999525
5-4  0.21296 -0.78862602  1.214546  0.9697200

```

Supplementary Figure 8

```

> TukeyHSD(res.aov3, which="strain")
  Tukey multiple comparisons of means
    95% family-wise confidence level

Fit: aov(formula = growth ~ strain + conc + strain:conc, data = rstudio)

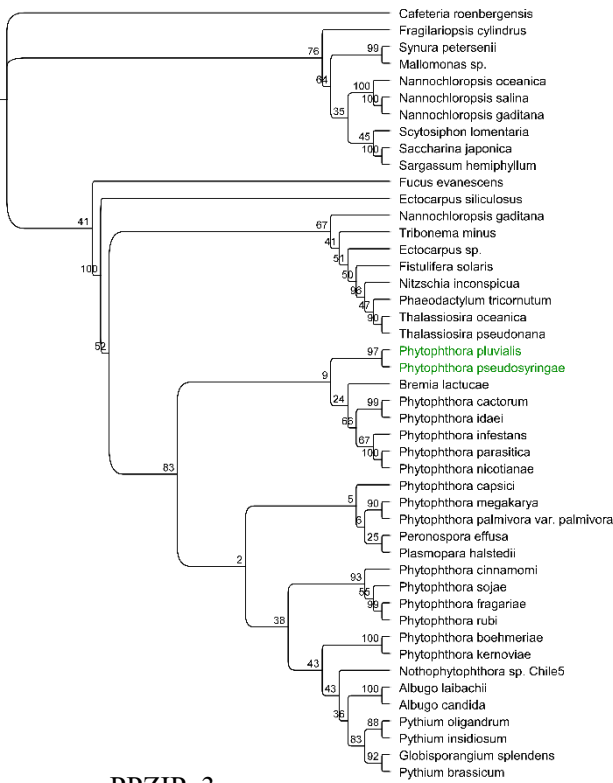
$strain
      diff          lwr          upr      p adj
3618-3000  7.15070  6.149114  8.152286  0.0000000
3632-3000  8.55770  7.556114  9.559286  0.0000000
3880-3000  5.55426  4.552674  6.555846  0.0000000
4015-3000 15.55906 14.557474 16.560646  0.0000000
3632-3618  1.40700  0.405414  2.408586  0.0030199
3880-3618 -1.59644 -2.598026 -0.594854  0.0007459
4015-3618  8.40836  7.406774  9.409946  0.0000000
3880-3632 -3.00344 -4.005026 -2.001854  0.0000000
4015-3632  7.00136  5.999774  8.002946  0.0000000
4015-3880 10.00480  9.003214 11.006386  0.0000000

```

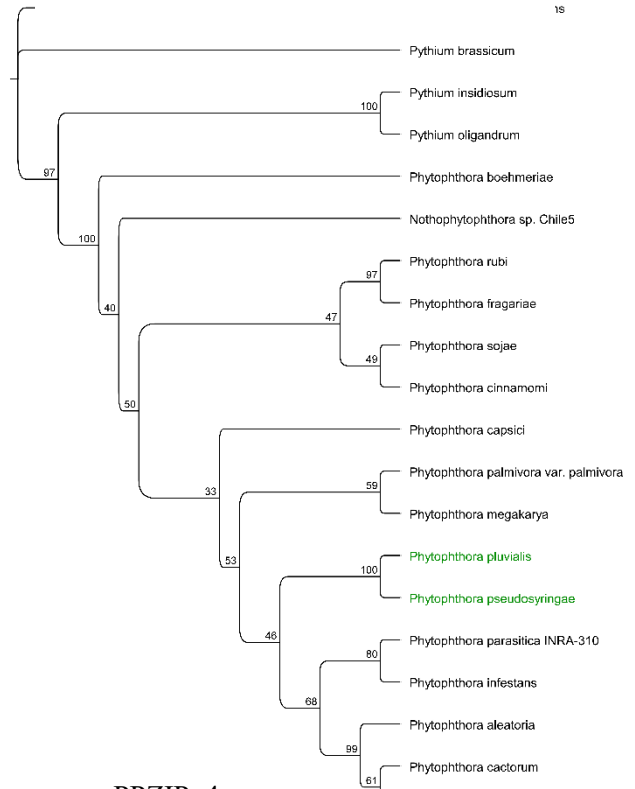
Supplementary Figure 9

Supplementary Figure 10

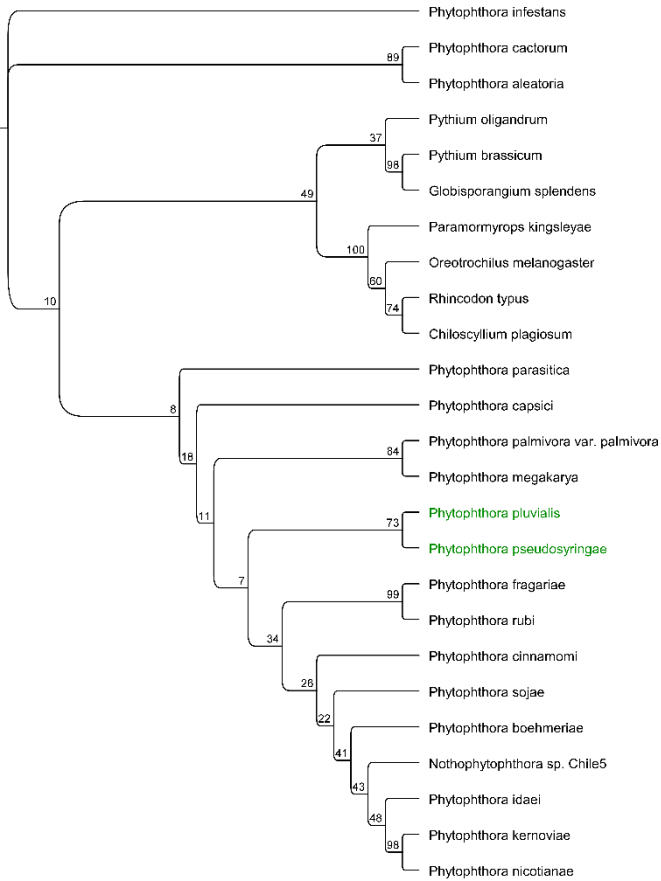
PPZIP_1



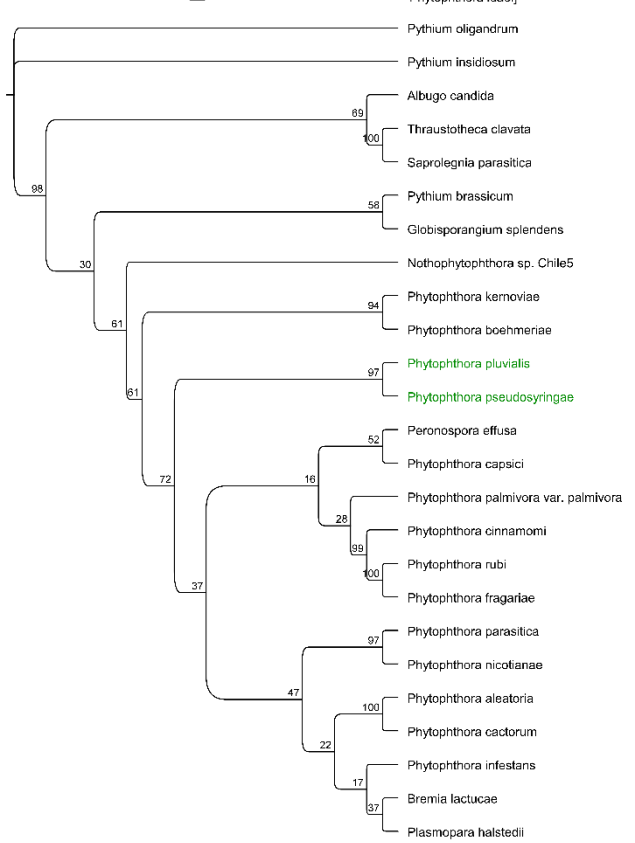
PPZIP_2



PPZIP_3

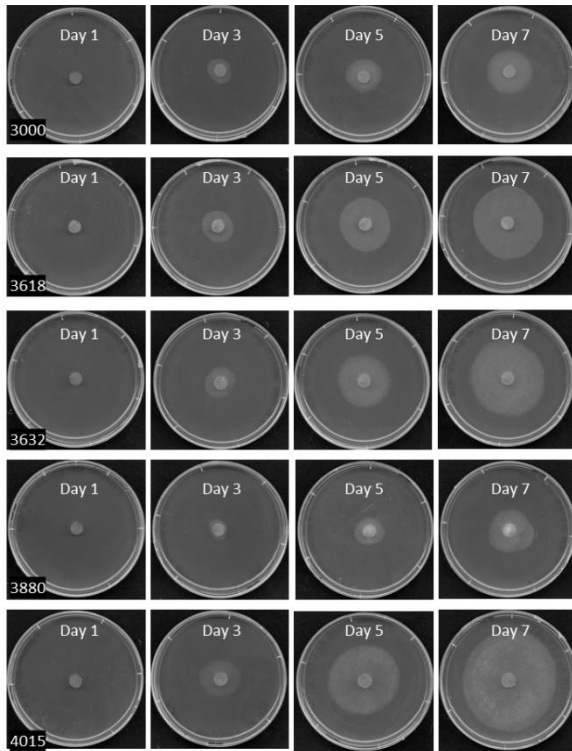


PPZIP_4

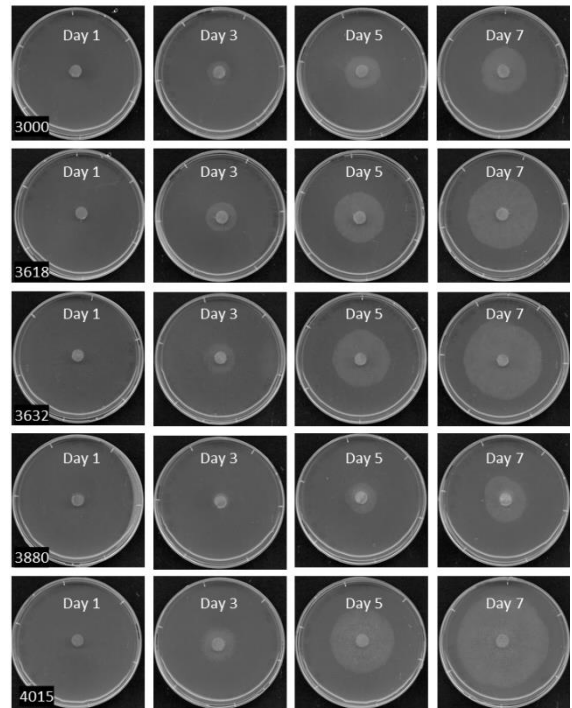


P. pluvialis mycelial growth at different temperatures

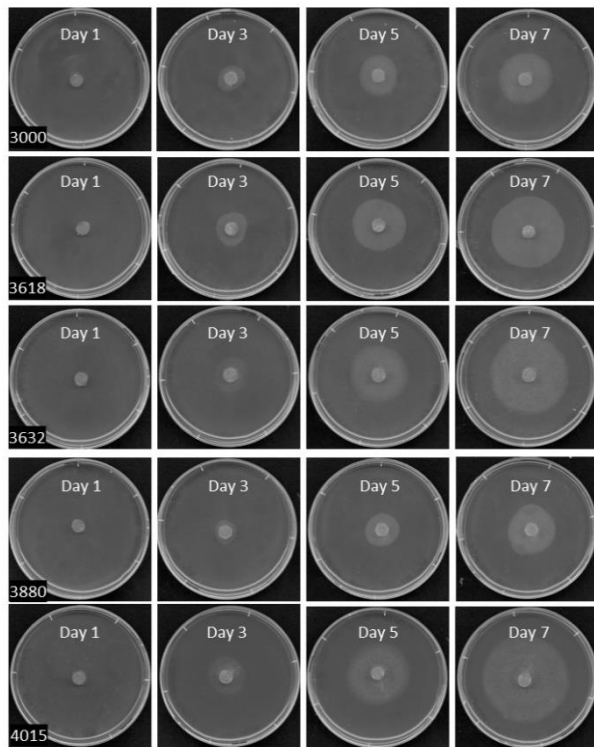
15 degrees- 3000



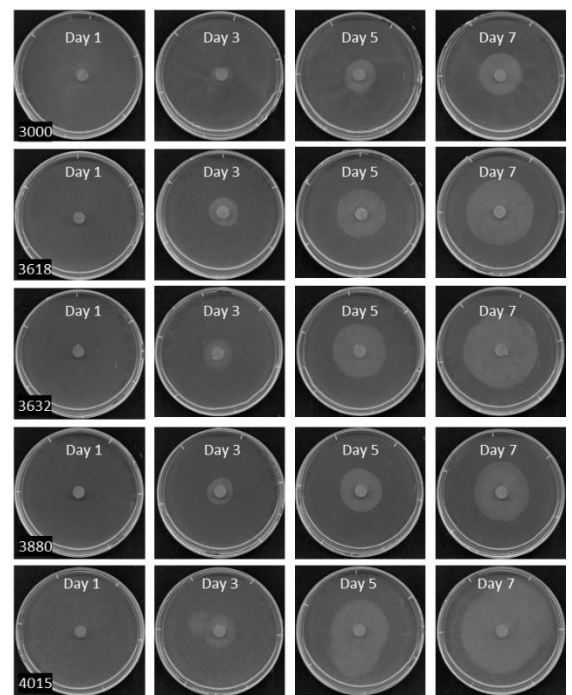
16 degrees



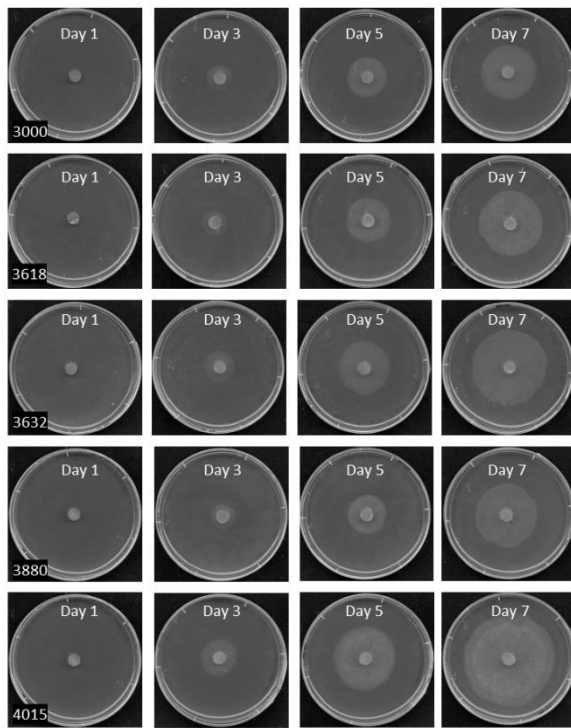
17 degrees



18 degrees



19 degrees



20 degrees

